SANDIA REPORT

SAND2009-5805
Unlimited Release
Printed September 2009

Efficient Algorithms for Mixed Aleatory-Epistemic Uncertainty Quantification with Application to Radiation-Hardened Electronics

Part I: Algorithms and Benchmark Results

Michael S. Eldred, Laura P. Swiler

Prepared by
Sandia National Laboratories
Albuquerque, New Mexico 87185 and Livermore, California 94550

Sandia is a multiprogram laboratory operated by Sandia Corporation,
a Lockheed Martin Company, for the United States Department of Energy's
National Nuclear Security Administration under Contract DE-AC04-94-AL85000.

Issued by Sandia National Laboratories, operated for the United States Department of Energy by Sandia Corporation.

Available to DOE and DOE contractors from
U.S. Department of Energy
Office of Scientific and Technical Information
P.O. Box 62
Oak Ridge, TN 37831

Telephone: (865) 576-8401
Facsimile: (865) 576-5728
E-Mail: reports@adonis.osti.gov
Online ordering: http://www.osti.gov/bridge

Available to the public from
U.S. Department of Commerce
National Technical Information Service
5285 Port Royal Rd
Springfield, VA 22161

Telephone: (800) 553-6847
Facsimile: (703) 605-6900
E-Mail: orders@ntis.fedworld.gov
Online ordering: http://www.ntis.gov/help/ordermethods.asp?loc=7-4-0#online

SAND2009-5805
Unlimited Release
Printed September 2009

Efficient Algorithms for Mixed Aleatory-Epistemic Uncertainty Quantification with Application to Radiation-Hardened Electronics

Part I: Algorithms and Benchmark Results

Michael S. Eldred, Laura P. Swiler
Optimization and Uncertainty Quantification Department

Sandia National Laboratories
P.O. Box 5800
Albuquerque, NM 87185

Abstract

This report documents the results of an FY09 ASC V&V Methods level 2 milestone demonstrating new algorithmic capabilities for mixed aleatory-epistemic uncertainty quantification. Through the combination of stochastic expansions for computing aleatory statistics and interval optimization for computing epistemic bounds, mixed uncertainty analysis studies are shown to be more accurate and efficient than previously achievable. Part I of the report describes the algorithms and presents benchmark performance results. Part II applies these new algorithms to UQ analysis of radiation effects in electronic devices and circuits for the QASPR program.

Contents

List of Figures

List of Tables

Executive Summary

Uncertainty quantification (UQ) is the process of determining the effect of input uncertainties on response metrics of interest. These input uncertainties may be characterized as either aleatory uncertainties, which are irreducible variabilities inherent in nature, or epistemic uncertainties, which are reducible uncertainties resulting from a lack of knowledge. Since sufficient data is generally available for aleatory uncertainties, input probability distributions can be defined and probabilistic methods are commonly used. Conversely, for epistemic uncertainties, data is generally too sparse to support probabilistic input descriptions, leading to nonprobabilistic approaches based on interval specifications.

For efficient computation of aleatory statistics, this report proposes the usage of collocation-based stochastic expansion methods. When employing optimal polynomial bases for problems with sufficient response smoothness, exponential convergence rates can be obtained for aleatory statistics with the use of methods such as polynomial chaos expansions and stochastic collocation. Compared to the relatively slow polynomial convergence rate ($\frac{1}{\sqrt{N}}$) of traditional sampling methods, stochastic expansions can demonstrate impressive advantages in efficiency. We explore approaches based on purely aleatory expansions as well as combined aleatory-epistemic expansions, where both approaches support derivatives of statistics with respect to the epistemic parameters.

Resolution of epistemic interval bounds through traditional sampling approaches suffers from the same slow $\frac{1}{\sqrt{N}}$ convergence rate. Since the desired minima and maxima of the output ranges are local point solutions in the epistemic parameter space (as opposed to integrated quantities), a more directed technique is to employ optimization methods to compute these extrema, resulting in more precise output bounds at lower cost. In this report, we explore the use of adaptive global optimization approaches based on expected improvement of Gaussian process models (for non-monotonic problems) as well as local gradient-based optimization approaches based on stochastic sensitivity analysis (for monotonic and potentially high dimensional problems), where as much information as possible is shared between the minimization and maximization subproblem computations.

When both aleatory and epistemic uncertainties are present, it is desirable to maintain a segregation between aleatory and epistemic sources within a nested analysis procedure known as second-order probability. Current production analyses for mixed UQ employ the use of nested sampling, where each sample taken from epistemic intervals at the outer loop results in an inner loop sampling over the aleatory probability distributions. For ASC-scale models of interest, nested sampling typi-

cally results in significantly under-resolved results, particularly at the epistemic outer loop. This under-resolution of epistemic intervals manifests itself as a nonconservative under-prediction of possible outcomes, which would be an important concern in mission-critical national security applications. By instead combining the stochastic expansion machinery for aleatory uncertainty with optimization-based interval estimation for epistemic uncertainty, the second-order probability approach becomes more tailored for the distinct goals at the different nested analysis levels, resulting in more efficient computation, more precise results, and greater overall confidence in the UQ assessment.

In Part I of this report, algebraic benchmark problems of differing dimensionality and smoothness are used to demonstrate the performance of these methods relative to nested sampling approaches. In these benchmarks, reductions of at least five orders of magnitude in simulation expense (100000x speedup) are demonstrated while simultaneously obtaining more precise results. The most effective and affordable approaches are then carried forward in mixed UQ studies for radiation-hardened electronics within the QASPR program in Part II of this report.

This milestone crosscuts multiple centers, drawing on capabilities for uncertainty analysis from DAKOTA (1410), device and circuit simulation from Charon and Xyce (1430), and QASPR data analysis, model development, and program relevance (0410, 1340, 1430, 1540). New capabilities developed for this milestone are being inserted into production UQ analysis procedures for current and future radiation effects studies, and this trend is expected to continue with V&V efforts in other program areas.

Chapter 1

Introduction

Uncertainty quantification (UQ) is the process of determining the effect of input uncertainties on response metrics of interest. These input uncertainties may be characterized as either aleatory uncertainties, which are irreducible variabilities inherent in nature, or epistemic uncertainties, which are reducible uncertainties resulting from a lack of knowledge. Since sufficient data is generally available for aleatory uncertainties, probabilistic methods are commonly used for computing response distribution statistics based on input probability distribution specifications. Conversely, for epistemic uncertainties, data is generally too sparse to support probabilistic input descriptions, leading to nonprobabilistic methods based on interval specifications.

1.1 Aleatory UQ

One technique for the analysis of aleatory uncertainties using probabilistic methods is the polynomial chaos expansion (PCE) approach to UQ. In this work, we start from a foundation of generalized polynomial chaos using the Wiener-Askey scheme [55], in which Hermite, Legendre, Laguerre, Jacobi, and generalized Laguerre orthogonal polynomials are used for modeling the effect of uncertain variables described by normal, uniform, exponential, beta, and gamma probability distributions, respectively[1]. These polynomial selections are optimal for these distribution types since they are orthogonal with respect to an inner product weighting function that corresponds (identical support range, weight differs by at most a constant factor) to the probability density functions for these continuous distributions. Orthogonal polynomials can be computed for any positive weight function, so these five classical orthogonal polynomials may be augmented with numerically-generated polynomials for other probability distributions; in particular, for the lognormal, loguniform, triangular, gumbel, frechet, weibull, and bin-based histogram distributions additionally supported by DAKOTA. When independent standard random variables are used (or computed through transformation), the variable expansions are uncoupled, allowing the polynomial orthogonality properties to be applied on a per-dimension basis. This allows one to mix and match the polynomial basis used for each variable without

[1]Orthogonal polynomial selections also exist for discrete probability distributions, but are not explored here.

interference with the spectral projection scheme for the response. With usage of the optimal basis corresponding to each the random variable types, exponential convergence rates can be obtained for statistics of interest.

In non-intrusive PCE, simulations are used as black boxes and the calculation of chaos expansion coefficients for response metrics of interest is based on a set of simulation response evaluations. To calculate these response PCE coefficients, two primary classes of approaches have been proposed: spectral projection and linear regression. The spectral projection approach projects the response against each basis function using inner products and employs the polynomial orthogonality properties to extract each coefficient. Each inner product involves a multidimensional integral over the support range of the weighting function, which can be evaluated numerically using sampling, quadrature, or sparse grid approaches. The linear regression approach (also known as point collocation or stochastic response surfaces) uses a single linear least squares solution to solve for the PCE coefficients which best match a set of response values obtained from a design of computer experiments.

Stochastic collocation (SC) is a second stochastic expansion approach that is closely related to PCE. Whereas PCE estimates coefficients for known orthogonal polynomial basis functions, SC forms Lagrange interpolation functions for known coefficients. Since the i^{th} interpolation function is 1 at collocation point i and 0 for all other collocation points, it is easy to see that the expansion coefficients are just the response values at each of the collocation points. The formation of multidimensional interpolants with this property requires the use of structured collocation point sets derived from tensor products or sparse grids. The key to the approach is performing collocation using the Gauss points and weights from the same optimal orthogonal polynomials used in PCE, which results in the same exponential convergence rates.

1.2 Stochastic Sensitivity Analysis

Once PCE or SC representations have been obtained for a response metric of interest, analytic expressions can be derived for the moments of the expansion (from integration over the aleatory/probabilistic random variables) and for the derivatives of these moments with respect to other nonprobabilistic variables, allowing for efficient design under uncertainty and mixed aleatory-epistemic UQ formulations involving moment control or bounding. In this report, we are interested in the latter, where bounds on moment-based metrics are computed using gradient-based interval estimation. This report presents two approaches for calculation of sensitivities of moments with respect to nonprobabilistic dimensions (design or epistemic), one involving response function expansions over both probabilistic and nonprobabilistic variables and one involving response derivative expansions over only the probabilistic variables. In the former case, the dimensionality of the expansions is increased (requiring increased simulation runs to construct them), but the technique remains zeroth-order and the expansion

spans the design/epistemic space (or potentially some subset of it). In the latter case, the expansion dimensionality is not increased, but accurate gradients with respect to the nonprobabilistic variables are now required for each simulation and the expansion over aleatory variables must be regenerated for each new design/epistemic point.

1.3 Mixed Aleatory-Epistemic UQ

A common approach to quantifying the effects of mixed aleatory and epistemic uncertainties is to perform second-order probability (SOP) analyses [23]. In SOP, we treat the aleatory and epistemic variables separately, and perform nested iteration, typically sampling epistemic variables on the outer loop, then sampling over aleatory variables on the inner loop. In this fashion, we generate families or ensembles of distributions, where each distribution represents the uncertainty generated by sampling over the aleatory variables. Given that the ensemble stems from multiple realizations of the epistemic uncertainties, the interpretation is that each distribution instance has no relative probability of occurrence, only that each instance is possible. For prescribed statistic on the response (such as a mean or percentile), an interval on that statistic of interest is computed based on the ensemble. This interval on a statistic is interpreted simply as a possible range, where the statistic could take any of the possible values in the range.

SOP can become computationally expensive when it is implemented using two nested sampling loops. However, the SOP procedure has the advantage that it is easy to separate and identify the aleatory vs. epistemic uncertainty. Each particular set of epistemic variable values generates an entire cumulative distribution function (CDF) for the response quantities based on the aleatory uncertainty. Plotting the entire ensemble of CDFs will allow one to visualize the upper and lower bound on the family of distributions (these plots are sometimes called horsetail plots since the CDFs overlaid on each other can resemble a horse's tail). Thus, a goal in this work is to preserve the advantages of uncertainty separation for purposes of visualization and interpretation, but address algorithmic issues with accuracy and efficiency of the SOP approach.

In this report, we propose a new approach for performing SOP analysis in which the inner-loop CDFs will be calculated using a stochastic expansion method, and the outer loop bounds will be computed with interval optimization. The advantages of this can be significant, due to several factors. First, the stochastic expansion methods can be much more efficient than sampling for calculation of a CDF (exponential convergence rates instead of $\frac{1}{\sqrt{N}}$ polynomial rate). Another advantage is the ability to compute analytic statistics and their derivatives using the stochastic sensitivity approaches. This enables efficient gradient-based local approaches (such as sequential quadratic programming) and nongradient-based global approaches (such as efficient global optimization) to computing response intervals through direct minimization

and maximization of the response over the range of the epistemic inputs. These optimization methods are more directed and will generally be more efficient than using random sampling to estimate the interval bounds. This interval estimation procedure is then used to define either the outer loop of a SOP approach or the cell computation component within the Dempster-Shafer theory of evidence approach.

1.4 Outline of Report

Chapter 2 describes the outer loop of local and global optimization-based interval estimation; Chapter 3 describes the inner loop of collocation-based stochastic expansion methods; Chapter 4 presents computational experiments using these methods for algebraic benchmark test problems; and Chapter 5 presents concluding remarks. Part II of this report includes additional computational results for UQ analysis of electronic devices and circuits for Sandia's QASPR program.

Chapter 2

The Outer Loop: Optimization-Based Interval Estimation

2.1 Epistemic Uncertainty Quantification

Epistemic uncertainty is sometimes referred to as state of knowledge uncertainty, subjective uncertainty, or reducible uncertainty, meaning that the uncertainty can be reduced through increased understanding (research), or increased and more relevant data [24]. There are a variety of approaches to propagating epistemic uncertainty, each of which differs significantly from traditional probabilistic propagation techniques.

The simplest way to propagate epistemic uncertainty is by interval analysis. In interval analysis, it is assumed that nothing is known about the uncertain input variables except that they lie within certain intervals. The problem of uncertainty propagation then becomes an interval analysis problem: given inputs that are defined within intervals, what is the corresponding interval on the outputs? Although interval analysis is conceptually simple, in practice it can be difficult to determine the more effective solution approach. A direct approach is to use optimization to find the maximum and minimum values of the output measure of interest, which correspond to the upper and lower interval bounds on the output, respectively. In practice, it may require a large number of function evaluations to determine these optima, especially if the simulation is very nonlinear with respect to the inputs, has a high number of inputs with interaction effects, exhibits discontinuities, etc.

Interval methods are only one approach to characterizing and modeling epistemic uncertainty. There are many others, including possibility theory, fuzzy set theory, and Dempster-Shafer evidence theory [23]. In this report, we focus primarily on interval methods, with some discussion of evidence theory.

We are interested in problems where all of the epistemic uncertain variables are characterized by intervals (a "pure" epistemic analysis) and in problems which have a mixtured of aleatory and epistemic uncertain inputs. In this mixed-case, we commonly

use a nested approach, where the "outer-loop" refers to treatment of the epistemic variables and the "inner-loop" refers to treatment of the aleatory variables. The segregation of epistemic and aleatory variables and their treatment by nested iteration is called second-order probability and is discussed in Section 2.3. We conclude this chapter with a discuss of Dempster-Shafer evidence theory in Section 2.4 and how the interval-based optimization methods discussed can be extended to this case.

2.2 Interval Optimization

This section presents a general formulation for determining interval bounds on the output measures of interest in the case of mixed epistemic-aleatory uncertainties. Given the capability to compute analytic statistics of the response along with design sensitivities of these statistics, we pursue optimization-based interval estimation approaches for epistemic and mixed aleatory-epistemic uncertainty quantification. We first present the optimization interval estimation process, followed by two UQ approaches in Sections 2.3 and 2.4 that may employ it.

Where applicable, we will employ derivatives of the statistics with respect to the nonprobabilistic parameters in order to guide optimization processes. But rather than performing a single minimization of an objective function subject to constraints as for OUU problems described in [14], we will solve two related bound-constrained problems:

$$\begin{aligned} &\text{minimize} && M(s) \\ &\text{subject to} && s_L \leq s \leq s_U \end{aligned} \tag{2.1}$$

$$\begin{aligned} &\text{maximize} && M(s) \\ &\text{subject to} && s_L \leq s \leq s_U \end{aligned} \tag{2.2}$$

where $M(s)$ is a metric of interest, probabilistic in the general mixed uncertainty case and deterministic in the pure epistemic case. That is, in the general case of mixed aleatory and epistemic variables, we are computing an interval on a statistic of a response function (mean, variance, or CDF/CCDF ordinate/abscissa), and in the pure epistemic case (no aleatory uncertain variables), we are computing an interval on the response function itself.

There are a number of algorithms that can solve these bound constrained optimization problems, which are categorized below as either simulation-based or surrogate-based methods and as either global, local, or sampling methods.

- Simulation-based methods interface directly with the calculation of the metric being optimized, without any surrogate model indirection.

  - Local gradient-based optimization solvers, such as bound-constrained Newton and quasi-Newton methods (see Section 2.2.1). Local optimization solvers are best for smooth monotonic problems as they require accurate, reliable sensitivities and do not guarantee the location of global optima. They do, however, scale to larger dimensional problems.
  - Global optimizers, such as multi-start local search, genetic algorithms, DIRECT, etc. These approaches can be very expensive, but have a much higher probability of locating global optima since they search the entire parameter domain.
  - Sampling methods, such as Latin hypercube sampling. This simple approach is not really an optimization algorithm; however it can estimate the upper and lower bounds of the response metric by sampling from the uncertain interval inputs and then taking the maximum and minimum from the set of output values obtained during the sampling process [45]. Usually a uniform distribution is assumed over the input intervals, although this is not necessary (if monotonicity in the response was probable, a distribution weighted more heavily at the input bounds would be preferred). Although uniform distributions may be used to create samples, one cannot assign a probabilistic distribution to them or make a corresponding probabilistic interpretation of the output. That is, one cannot make a CDF of the output: all one can assume is that sample input values were generated, corresponding sample output values were created, and the minimum and maximum of the output are the estimated output interval bounds. This sampling approach is easy to implement, but its accuracy is highly dependent on the number of samples. Often, sampling will generate output bounds which underestimate the true output interval.

- Surrogate-based methods employ inexpensive approximations (e.g., polynomial regression, neural nets, adaptive splines, kriging, etc.) to the true metric being optimized in order to smooth noisy response functions, capture trends, and reduce expense. The expense of these methods is dominated by the cost of constructing and updating the surrogate models.

  - Local methods, such as first-order trust region model management based on data fits, multifidelity models, or reduced-order models [13].
  - Global methods, such as efficient global optimization (see Section 2.2.2).
  - Sampling methods, such as Latin hypercube sampling. This approach starts with coarse sampling and uses these samples to create a surrogate model. The surrogate model can then be sampled very extensively (e.g. a million times) to obtain upper and lower bound estimates.

At the interval estimation level, a key to computational efficiency is reusing as much information as possible within the solution procedures for these two related optimization problems. For gradient-based local approaches, we may only be able to reuse the

evaluation of aleatory statistics and their derivatives at the initial epistemic point. For nongradient-based global approaches, however, we will make significant reuse of surrogate model interpolation (EGO) and box partitioning (DIRECT) data. In addition, the same OUU machinery that we have developed in DAKOTA for bi-level, sequential, and multifidelity approaches [14] can be applied to reduce expense. At the aleatory UQ level, a key issue is the use of combined variable expansions over both epistemic and aleatory parameters (see Section 3.4.2.4) versus the use of expansions over only the aleatory parameters for each instance of the epistemic parameters (see Section 3.4.2.3). In this report, we focus on four combinations: bi-level nongradient-based global interval estimation employing combined and aleatory expansions and bi-level gradient-based local interval estimation employing combined and aleatory expansions along with their stochastic sensitivities.

In the following sections, we discuss specific optimization methods for interval estimation in greater detail; in particular, local gradient-based methods and the efficient global optimization approach (based on adaptive refinement of a Gaussian process surrogate model by a global optimizer) to interval estimation.

2.2.1 Local Optimization

Gradient-based algorithms are typically very efficient optimization methods. However, their performance depends on having accurate gradients, and they usually only guarantee finding local optima. In the case of "pure" interval optimization, where we are trying determine output bounds only as a function of interval epistemic variables, the gradient of the response measures with respect to the epistemic variables is required. In the case of mixed aleatory-epistemic problems, the gradient of the inner-loop statistical measures (e.g. functions of the aleatory variables) with respect to the epistemic variables is required. One advantage of the stochastic expansion methods as compared with plain sampling methods for the inner loop calculations is that the expansion methods do allow the formulation of analytic gradients of statistical moments with respect to epistemic variables.

In DAKOTA, we offer two main approaches for gradient-based interval optimization, although others may be used. The first algorithm is a Sequential Quadratric Programming (SQP) implementation that is part of the NPSOL library [21]. SQP algorithms are nonlinear programming techniques which use Newton's method to solve the Karush-Kuhn-Tucker first order necessary conditions for optimality based on a Lagrangian function. The second algorithm is a nonlinear interior point method which uses a quasi-Newton solver that is part of the OPT++ library [32]. Since Eqs. 2.1-2.2 do not include general nonlinear constraints, the distinction between the two methods is subtle and both are basically quasi-Newton methods based on BFGS updating.

2.2.2 Efficient Global Optimization

Many of the simulation models used for uncertainty analysis are very expensive in terms of computational cost. In this situation, we cannot afford to run the simulation model hundreds or thousands of times as part of an optimization to determine output interval bounds when the inputs are characterized by intervals. Instead, surrogate methods (also called meta-models or response-surfaces) are used. We use an optimization approach based on a method called Efficient Global Optimization (EGO) developed in [Jones, Schonlau, and Welch] [28]. EGO relies on a Gaussian process surrogate mode. EGO was developed to facilitate the unconstrained minimization of expensive implicit response functions. The idea in EGO is to use properties of the Gaussian process (specifically, the predicted variance in the estimate at potential points in the space) to balance exploitation of existing good solutions with exploration of parts of the domain which are sparsely populated and where a potential optimum could be located.

The method builds an initial Gaussian process model as a global surrogate for the response function, then adaptively selects additional samples to be included in the Gaussian process model in subsequent iterations. The new samples are selected based on how much they are expected to improve the current best solution to the optimization problem using a criteria coded into an expected improvement function (EIF). There are a number of variations on the concept of using a Gaussian process surrogate in optimization, including [30], [27], and [4].

We have taken the EGO concept and have adapted it for interval estimation in order to allow reuse of data between the minimization and maximization subproblems. We first build the GP for function minimization, then we take the existing points generated by that process, change the objective function and expected improvement function to perform function maximization, and then reuse the same GP to find the maximum response value. We have found this approach to be very efficient, where the majority of true function evaluations of the simulation model are performed in finding the function minimum, and only a few additional samples are added to the GP to find the function maximum. The performance of this EGO-based interval optimization will depend on the nonlinearity of the simulation model and the number of input dimensions. We have seen it perform very well relative to other surrogate-based methods on low dimensional problems. For example, the EGO method based on an adaptive surrogate model can often find minimum and maximum estimates of the output measures based on 30-40 function evaluations whereas optimization performed on a surrogate constructed on a fixed sample set may require a hundred samples or more.

The basic outline of the EGO algorithm is as follows:

1. Generate a Latin Hypercube sample (LHS) over the input points, and evaluate the objective function by running the simulation model at these points.

2. Build an initial Gaussian process model of the objective function.

3. Find the point that maximizes the EIF. If the EIF value at this point is sufficiently small, stop.

4. Evaluate the objective function at the point where the EIF is maximized. Update the Gaussian process model using this new point. Go to Step 2.

We augment the procedure above by a few more steps. After the point is found which minimizes the EIF (corresponding to the minimum of the function over the domain),we then take all of the true function evaluations (e.g. simulation runs) from the minimization step and reuse them within another GP search where we switch the sign of the expected improvement function so that we are maximizing the function. These subseqent steps are:

5. Redefine the EIF to indicate function maximization, not minimization. Note that the GP itself is unchanged.

6. Find the point that maximizes the EIF. If the EIF value at this point is sufficiently small, stop.

7. Evaluate the objective function at the point where the EIF is maximized. Update the Gaussian process model using this new point. Go to Step 6.

The next subsections describe the Gaussian process and the expected improvement function that we used in more detail. The DIRECT optimizer is also briefly described.

2.2.2.1 Gaussian Process Model

Gaussian process (GP) models differ from most other surrogate models because they provide not just a predicted value at an unsampled point, but also and estimate of the prediction variance. This variance gives an indication of the uncertainty in the GP model, which results from the construction of the covariance function. This function is based on the idea that when input points are near one another, the correlation between their corresponding outputs will be high. As a result, the uncertainty associated with the model's predictions will be small for input points which are near the points used to train the model, and will increase as one moves further from the training points.

It is assumed that the true response function being modeled $G(\mathbf{u})$ can be described by: [4]

$$G(\mathbf{u}) = \mathbf{h}(\mathbf{u})^T \boldsymbol{\beta} + Z(\mathbf{u}) \tag{2.3}$$

where $\mathbf{h}()$ is the trend of the model, $\boldsymbol{\beta}$ is the vector of trend coefficients, and $Z()$ is a stationary Gaussian process with zero mean (and covariance defined below) that describes the departure of the model from its underlying trend. The trend of the

model can be assumed to be any function. We use a quadratic trend function, but a constant value is often assumed to be sufficient [38].

The covariance between outputs of the Gaussian process $Z()$ at points $\mathbf{a}$ and $\mathbf{b}$ is defined as:

$$Cov\left[Z(\mathbf{a}), Z(\mathbf{b})\right] = \sigma_Z^2 R(\mathbf{a}, \mathbf{b}) \tag{2.4}$$

where σ_Z^2 is the process variance and $R()$ is the correlation function. There are several options for the correlation function, but the squared-exponential function is common [38], and is used here for $R()$:

$$R(\mathbf{a}, \mathbf{b}) = \exp\left[-\sum_{i=1}^{d} \theta_i (a_i - b_i)^2\right] \tag{2.5}$$

where d represents the dimensionality of the problem (the number of random variables), and θ_i is a scale parameter that indicates the correlation between the points within dimension i. A large θ_i is representative of a short correlation length.

The expected value $\mu_G()$ and variance $\sigma_G^2()$ of the GP model prediction at point $\mathbf{u}$ are:

$$\mu_G(\mathbf{u}) = \mathbf{h}(\mathbf{u})^T \boldsymbol{\beta} + \mathbf{r}(\mathbf{u})^T \mathbf{R}^{-1}(\mathbf{g} - \mathbf{F}\boldsymbol{\beta}) \tag{2.6}$$

$$\sigma_G^2(\mathbf{u}) = \sigma_Z^2 - \begin{bmatrix}\mathbf{h}(\mathbf{u})^T & \mathbf{r}(\mathbf{u})^T\end{bmatrix} \begin{bmatrix}\mathbf{0} & \mathbf{F}^T \\ \mathbf{F} & \mathbf{R}\end{bmatrix}^{-1} \begin{bmatrix}\mathbf{h}(\mathbf{u}) \\ \mathbf{r}(\mathbf{u})\end{bmatrix} \tag{2.7}$$

where $\mathbf{r}(\mathbf{u})$ is a vector containing the covariance between $\mathbf{u}$ and each of the n training points (defined by Eq. 2.4), $\mathbf{R}$ is an $n \times n$ matrix containing the correlation between each pair of training points, $\mathbf{g}$ is the vector of response outputs at each of the training points, and $\mathbf{F}$ is an $n \times q$ matrix with rows $\mathbf{h}(\mathbf{u}_i)^T$ (the trend function for training point i containing q terms; for a constant trend $q = 1$). This form of the variance accounts for the uncertainty in the trend coefficients $\boldsymbol{\beta}$, but assumes that the parameters governing the covariance function (σ_Z^2 and $\boldsymbol{\theta}$) have known values. The parameters σ_Z^2 and $\boldsymbol{\theta}$ are determined through maximum likelihood estimation. This involves taking the log of the probability of observing the response values $\mathbf{g}$ given the covariance matrix $\mathbf{R}$, which can be written as: [38]

$$\log\left[p(\mathbf{g}|\mathbf{R})\right] = -\frac{1}{n}\log|\mathbf{R}| - \log(\hat{\sigma}_Z^2) \tag{2.8}$$

where $|\mathbf{R}|$ indicates the determinant of $\mathbf{R}$, and $\hat{\sigma}_Z^2$ is the optimal value of the variance given an estimate of $\boldsymbol{\theta}$ and is defined by:

$$\hat{\sigma}_Z^2 = \frac{1}{n}(\mathbf{g} - \mathbf{F}\boldsymbol{\beta})^T \mathbf{R}^{-1}(\mathbf{g} - \mathbf{F}\boldsymbol{\beta}) \tag{2.9}$$

Maximizing Eq. 2.8 gives the maximum likelihood estimate of $\boldsymbol{\theta}$, which in turn defines σ_Z^2. We use an iterative procedure defined in John McFarland's dissertation [31] to calculate the $\boldsymbol{\beta}$, $\boldsymbol{\theta}$, and σ_Z^2 parameters which define the GP. We use a global solver, DIRECT, to find these optimal parameters.

2.2.2.2 Expected Improvement Function

The expected improvement function is used to select the location at which a new training point should be added. The EIF is defined as the expectation that any point in the search space will provide a better solution than the current best solution based on the expected values and variances predicted by the GP model. An important feature of the EIF is that it provides a balance between exploiting areas of the design space where good solutions have been found, and exploring areas of the design space where the uncertainty is high. First, recognize that at any point in the design space, the GP prediction $\hat{G}()$ is a Gaussian distribution:

$$\hat{G}(\mathbf{u}) \sim N\left[\mu_G(\mathbf{u}), \sigma_G(\mathbf{u})\right] \tag{2.10}$$

where the mean $\mu_G()$ and the variance $\sigma_G^2()$ were defined in Eqs. 2.6 and 2.7, respectively. The EIF is defined as: [28]

$$EI\big(\hat{G}(\mathbf{u})\big) \equiv E\left[\max\Big(G(\mathbf{u}^*) - \hat{G}(\mathbf{u}), 0\Big)\right] \tag{2.11}$$

where $G(\mathbf{u}^*)$ is the current best solution chosen from among the true function values at the training points (henceforth referred to as simply G^*). This expectation can then be computed by integrating over the distribution $\hat{G}(\mathbf{u})$ with G^* held constant:

$$EI\big(\hat{G}(\mathbf{u})\big) = \int_{-\infty}^{G^*} (G^* - G)\ \hat{G}(\mathbf{u})\ dG \tag{2.12}$$

where G is a realization of $\hat{G}$. This integral can be expressed analytically as: [28]

$$EI\big(\hat{G}(\mathbf{u})\big) = (G^* - \mu_G)\ \Phi\left(\frac{G^* - \mu_G}{\sigma_G}\right) + \sigma_G\, \phi\left(\frac{G^* - \mu_G}{\sigma_G}\right) \tag{2.13}$$

where it is understood that μ_G and σ_G are functions of $\mathbf{u}$. The point at which the EIF is maximized is selected as an additional training point. With the new training point added, a new GP model is built and then used to construct another EIF, which is then used to choose another new training point, and so on, until the value of the EIF at its maximized point is below some specified tolerance. In [27] this maximization is performed using a Nelder-Mead simplex approach, which is a local optimization method. Because the EIF is often highly multimodal, it is expected that Nelder-Mead may fail to converge to the true global optimum. In [28], a branch-and-bound technique for maximizing the EIF is used, but was found to often be too expensive to run to convergence. In this report, an implementation of the DIRECT global optimization algorithm is used [17]. The DIRECT (DIviding RECTangles) algorithm is a derivative free global optimization method that balances local search in promising areas of the space with global search in unexplored regions. DIRECT adaptively subdivides the space of feasible design points (into smaller hyperrectangles) so as to guarantee that iterates are generated in the neighborhood of a global minimum in finitely many iterations. We use Joerg Gablonsky's implementation of DIRECT.

It is important to understand how the use of this EIF leads to optimal solutions. Eq. 2.13 indicates how much the objective function value at $\mathbf{x}$ is expected to be less than the predicted value at the current best solution. Because the GP model provides a Gaussian distribution at each predicted point, expectations can be calculated. Points with good expected values and even a small variance will have a significant expectation of producing a better solution (exploitation), but so will points that have relatively poor expected values and greater variance (exploration).

2.3 Second-order probability

In second-order probability [44] (SOP), we segregate the aleatory and epistemic variables and perform nested iteration, with aleatory analysis on the inner loop and epistemic analysis on the outer loop [23]. Starting from a specification of intervals and probability distributions on the inputs (as described in Section 3.4.2.5, the intervals may augment the probability distributions, insert into the probability distributions, or some combination), we generate an ensemble of CDF/CCDF probabilistic results, one CDF/CCDF result for each aleatory analysis. Given that the ensemble stems from multiple realizations of the epistemic uncertainties, the interpretation is that each CDF/CCDF instance has no relative probability of occurrence, only that each instance is possible. For prescribed response levels on the CDF/CCDF, an interval on the probability is computed based on the bounds of the horse tail at that level, and vice versa for prescribed probability levels.

Second-order probability may be expensive since it is often implemented with two sampling loops. However, it has the advantage that it is easy to separate and identify the aleatory vs. epistemic uncertainty. Each particular set of epistemic variable values generates an entire CDF/CCDF for the response quantities based on the aleatory uncertainty. So, for example, if one had 50 values or samples taken of the epistemic variables, one would have 50 CDFs. Plotting the entire ensemble of CDFs will allow one to see the upper and lower bound on the family of distributions. Plots of ensembles of CDFs generated in second-order probability analysis are sometimes called horsetail plots since the CDFs overlaid on each other can resemble a horse's tail.

In this report, we propose a new approach for performing second-order probability analysis. In this approach, the inner-loop CDFs will be calculated using a stochastic expansion method, and the outer loop bounds will be performed via interval optimization. The advantages of this can be significant, due to several factors. The first is that the stochastic expansion methods can be much more efficient than sampling for calculation of a CDF (exponential convergence rates instead of $\frac{1}{\sqrt{N}}$ polynomial rate). The second advantage is that stochastic expansion methods allow analytic representation of the moments and the derivatives of the moments with respect to the epistemic variables in the outer loop can be written analytically. These analytic derivatives can then be used within optimization methods to find interval bounds on

mean and variance, for example. Finally, the optimization methods in the outer loop are more directed and will often be more efficient than generating outer loop samples to estimate outer loop bounds.

2.4 Dempster-Shafer

In the Dempster-Shafer theory of evidence [44] (DSTE) approach, we start from a set of basic probability assignments (BPAs) for the epistemic uncertain variables, typically derived from a process of expert elicitation. These BPAs define sets of intervals for each epistemic variable, and for each possible combination of these intervals among the variables, we solve minimization and maximization problems for the interval of the response. These intervals define belief and plausibility functions that bound the true probability distribution of the response.

More specifically, each input variable may be defined by one or more intervals. The user assigns a basic probability assignment (BPA) to each interval, indicating how likely it is that the uncertain input falls within the interval. The BPAs for a particular uncertain input variable must sum to one. The intervals may be overlapping, contiguous, or have gaps. Dempster-Shafer has two measures of uncertainty, belief and plausibility. The intervals are propagated to calculate belief (a lower bound on a probability value that is consistent with the evidence) and plausibility (an upper bound on a probability value that is consistent with the evidence). Together, belief and plausibility define an interval-valued probability distribution on the results, not a single probability distribution.

The main method for calculating Dempster-Shafer belief structures is computationally very expensive. Typically, hundreds of thousands of samples are taken over the space. Each combination of input variable intervals defines an input " cell." [25] By interval combination, we mean the first interval of the first variable paired with the first interval for the second variable, etc. Within each interval calculation, it is necessary to find the minimum and maximum function value for that interval "cell." These minimum and maximum values are aggregated to create the belief and plausibility curves. The accuracy of the Dempster-Shafer results is highly dependent on the number of samples and the number of interval combinations. If one has many interval cells and few samples, the estimates for the minimum and maximum function evaluations are likely to be poor. The Dempster-Shafer method may use a surrogate model and/or optimization methods. We have extended the interval-optimization methods defined in Section 2.2.2 to Dempster-Shafer calculations with promising results [47].

Dempster-Shafer evidence theory is an attractive approach to propagation of evidence theory when using computational simulations, in part because it is a generalization of classical probability theory which allows the simulation code to remain black-box (it is non-intrusive to the code) and because the Dempster-Shafer calculations use much

of the probabilistic framework that exists in most places [24].

Dempster-Shafer theory is generally considered an approach for treating epistemic uncertainties. When aleatory uncertainties are also present, we may choose either to discretize the aleatory probability distributions into sets of intervals and treat them as well-characterized epistemic variables, or we may choose to segregate the aleatory uncertainties and treat them within an inner loop. In this latter case, DSTE can be seen as a generalization of SOP, in that the SOP interval minimization and maximization process is performed repeatedly for each "cell" defined by the BPAs in the DSTE analysis. As for SOP, this nested DSTE analysis reports intervals on statistics, and in particular, belief and plausibility results for statistics that are consistent with the epistemic evidence.

Chapter 3

The Inner Loop: Stochastic Expansion Methods

3.1 Polynomial Basis

3.1.1 Orthogonal polynomials in the Askey scheme

Table 3.1 shows the set of polynomials which provide an optimal basis for different continuous probability distribution types. It is derived from the family of hypergeometric orthogonal polynomials known as the Askey scheme [2], for which the Hermite polynomials originally employed by Wiener [50] are a subset. The optimality of these basis selections derives from their orthogonality with respect to weighting functions that correspond to the probability density functions (PDFs) of the continuous distributions when placed in a standard form. The density and weighting functions differ by a constant factor due to the requirement that the integral of the PDF over the support range is one.

Table 3.1. Linkage between standard forms of continuous probability distributions and Askey scheme of continuous hyper-geometric polynomials.

Distribution	Density function	Polynomial	Weight function	Support range
Normal	$\frac{1}{\sqrt{2\pi}} e^{\frac{-x^2}{2}}$	Hermite $He_n(x)$	$e^{\frac{-x^2}{2}}$	$[-\infty, \infty]$
Uniform	$\frac{1}{2}$	Legendre $P_n(x)$	1	$[-1, 1]$
Beta	$\frac{(1-x)^\alpha (1+x)^\beta}{2^{\alpha+\beta+1} B(\alpha+1, \beta+1)}$	Jacobi $P_n^{(\alpha,\beta)}(x)$	$(1-x)^\alpha (1+x)^\beta$	$[-1, 1]$
Exponential	e^{-x}	Laguerre $L_n(x)$	e^{-x}	$[0, \infty]$
Gamma	$\frac{x^\alpha e^{-x}}{\Gamma(\alpha+1)}$	Gen. Laguerre $L_n^{(\alpha)}(x)$	$x^\alpha e^{-x}$	$[0, \infty]$

Note that Legendre is a special case of Jacobi for $\alpha = \beta = 0$, Laguerre is a special case of generalized Laguerre for $\alpha = 0$, $\Gamma(a)$ is the Gamma function which extends the factorial function to continuous values, and $B(a, b)$ is the Beta function defined as $B(a, b) = \frac{\Gamma(a)\Gamma(b)}{\Gamma(a+b)}$. Some care is necessary when specifying the α and β parameters

for the Jacobi and generalized Laguerre polynomials since the orthogonal polynomial conventions [1] differ from the common statistical PDF conventions. The former conventions are used in Table 3.1.

3.1.2 Numerically generated orthogonal polynomials

If all random inputs can be described using independent normal, uniform, exponential, beta, and gamma distributions, then generalized PCE can be directly applied. If correlation or other distribution types are present, then additional techniques are required. One solution is to employ nonlinear variable transformations as described in Section 3.2.3 such that an Askey basis can be applied in the transformed space. This can be effective as shown in [15], but convergence rates are typically degraded. In addition, correlation coefficients are warped by the nonlinear transformation [7], and transformed correlation values are not always readily available. An alternative is to numerically generate the orthogonal polynomials, along with their Gauss points and weights, that are optimal for given random variable sets having arbitrary probability density functions [18, 22]. This preserves the exponential convergence rates for UQ applications with general probabilistic inputs, but performing this process for general joint density functions with correlation is a topic on ongoing research.

Figure 3.1 demonstrates the use of a numerically-generated basis for Rosenbrock's function, a simple fourth-order polynomial. For two lognormal random variable inputs (iid with mean = 1. and standard deviation = 0.5), we employ two basis selections: (1) PCE and SC employ a Hermite basis in a transformed standard normal space (blue curves), (2) polynomials that are orthogonal with respect to these lognormal PDFs are numerically generated (red curves). It is evident that exact results are obtained with a fourth-order expansion for the numerically-generated case, whereas the nonlinear variable transformation introduces additional nonlinearity that requires a much higher order expansion to accurately resolve. However, it is not always the case that a variable transformation increases the degree of nonlinearity; for the two rational functions presented in Chapter 4, this trend is reversed.

3.1.3 Interpolation polynomials

Lagrange polynomials interpolate a set of points in a single dimension using the functional form

$$L_j = \prod_{\substack{k=1 \\ k \neq j}}^{m} \frac{\xi - \xi_k}{\xi_j - \xi_k} \tag{3.1}$$

where it is evident that L_j is 1 at $\xi = \xi_j$, is 0 for each of the points $\xi = \xi_k$, and has order $m - 1$.

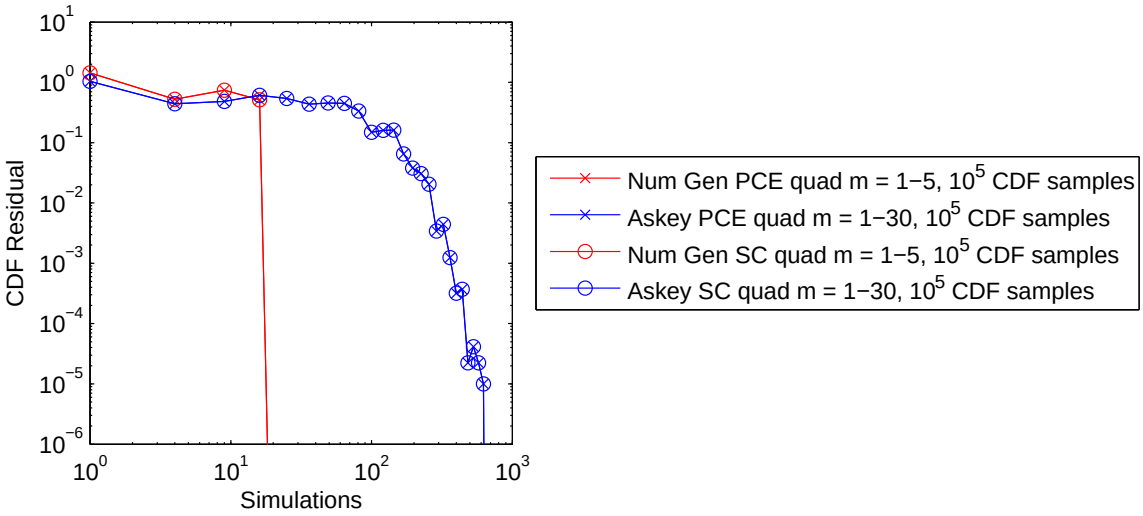

Figure 3.1. PCE and SC comparing Askey and numerically-generated basis for the Rosenbrock test problem with two lognormal variables.

For interpolation of a response function R in one dimension over m points, the expression

$$R(\xi) \cong \sum_{j=1}^{m} r(\xi_j)\, L_j(\xi) \tag{3.2}$$

reproduces the response values $r(\xi_j)$ at the interpolation points and smoothly interpolates between these values at other points. For interpolation in multiple dimensions, a tensor-product approach is used wherein

$$R(\boldsymbol{\xi}) \cong \sum_{j_1=1}^{m_{i_1}} \cdots \sum_{j_n=1}^{m_{i_n}} r\left(\xi_{j_1}^{i_1}, \ldots, \xi_{j_n}^{i_n}\right) \left(L_{j_1}^{i_1} \otimes \cdots \otimes L_{j_n}^{i_n}\right) = \sum_{j=1}^{N_p} r_j(\boldsymbol{\xi}) \boldsymbol{L}_j(\boldsymbol{\xi}) \tag{3.3}$$

where $\boldsymbol{i} = (m_1, m_2, \cdots, m_n)$ are the number of nodes used in the n-dimensional interpolation and $\xi_{j_l}^{i_k}$ is the j_l-th point in the k-th direction. As will be seen later (Section 3.3.1.3), interpolation on sparse grids involves a summation of these tensor products with varying $\boldsymbol{i}$ levels.

3.2 Stochastic Expansion Methods

3.2.1 Generalized Polynomial Chaos

The set of polynomials from Sections 3.1.1 and 3.1.2 are used as an orthogonal basis to approximate the functional form between the stochastic response output and each

of its random inputs. The chaos expansion for a response R takes the form

$$R = a_0 B_0 + \sum_{i_1=1}^{\infty} a_{i_1} B_1(\xi_{i_1}) + \sum_{i_1=1}^{\infty} \sum_{i_2=1}^{i_1} a_{i_1 i_2} B_2(\xi_{i_1}, \xi_{i_2}) + \sum_{i_1=1}^{\infty} \sum_{i_2=1}^{i_1} \sum_{i_3=1}^{i_2} a_{i_1 i_2 i_3} B_3(\xi_{i_1}, \xi_{i_2}, \xi_{i_3}) + ... \tag{3.4}$$

where the random vector dimension is unbounded and each additional set of nested summations indicates an additional order of polynomials in the expansion. This expression can be simplified by replacing the order-based indexing with a term-based indexing

$$R = \sum_{j=0}^{\infty} \alpha_j \Psi_j(\boldsymbol{\xi}) \tag{3.5}$$

where there is a one-to-one correspondence between $a_{i_1 i_2 ... i_n}$ and α_j and between $B_n(\xi_{i_1}, \xi_{i_2}, ..., \xi_{i_n})$ and $\Psi_j(\boldsymbol{\xi})$. Each of the $\Psi_j(\boldsymbol{\xi})$ are multivariate polynomials which involve products of the one-dimensional polynomials. For example, a multivariate Hermite polynomial $B(\boldsymbol{\xi})$ of order n is defined from

$$B_n(\xi_{i_1}, ..., \xi_{i_n}) = e^{\frac{1}{2}\boldsymbol{\xi}^T \boldsymbol{\xi}} (-1)^n \frac{\partial^n}{\partial \xi_{i_1} ... \partial \xi_{i_n}} e^{-\frac{1}{2}\boldsymbol{\xi}^T \boldsymbol{\xi}} \tag{3.6}$$

which can be shown to be a product of one-dimensional Hermite polynomials involving a multi-index m_i^j:

$$B_n(\xi_{i_1}, ..., \xi_{i_n}) = \Psi_j(\boldsymbol{\xi}) = \prod_{i=1}^{n} \psi_{m_i^j}(\xi_i) \tag{3.7}$$

3.2.1.1 Expansion truncation and tailoring

In practice, one truncates the infinite expansion at a finite number of random variables and a finite expansion order

$$R \cong \sum_{j=0}^{P} \alpha_j \Psi_j(\boldsymbol{\xi}) \tag{3.8}$$

Traditionally, the polynomial chaos expansion includes a complete basis of polynomials up to a fixed total-order specification. For example, the multidimensional basis polynomials for a second-order expansion over two random dimensions are

$$\begin{array}{rcccl}
\Psi_0(\boldsymbol{\xi}) & = & \psi_0(\xi_1)\, \psi_0(\xi_2) & = & 1 \\
\Psi_1(\boldsymbol{\xi}) & = & \psi_1(\xi_1)\, \psi_0(\xi_2) & = & \xi_1 \\
\Psi_2(\boldsymbol{\xi}) & = & \psi_0(\xi_1)\, \psi_1(\xi_2) & = & \xi_2 \\
\Psi_3(\boldsymbol{\xi}) & = & \psi_2(\xi_1)\, \psi_0(\xi_2) & = & \xi_1^2 - 1 \\
\Psi_4(\boldsymbol{\xi}) & = & \psi_1(\xi_1)\, \psi_1(\xi_2) & = & \xi_1 \xi_2 \\
\Psi_5(\boldsymbol{\xi}) & = & \psi_0(\xi_1)\, \psi_2(\xi_2) & = & \xi_2^2 - 1
\end{array}$$

The total number of terms N_t in an expansion of total order p involving n random variables is given by

$$N_t \;=\; 1 + P \;=\; 1 + \sum_{s=1}^{p} \frac{1}{s!} \prod_{r=0}^{s-1} (n+r) \;=\; \frac{(n+p)!}{n!p!} \tag{3.9}$$

This traditional approach will be referred to as a "total-order expansion."

An important alternative approach is to employ a "tensor-product expansion," in which polynomial order bounds are applied on a per-dimension basis (no total-order bound is enforced) and all combinations of the one-dimensional polynomials are included. In this case, the example basis for $p = 2, n = 2$ is

$$\begin{aligned}
\Psi_0(\boldsymbol{\xi}) &= \psi_0(\xi_1)\,\psi_0(\xi_2) &&= 1 \\
\Psi_1(\boldsymbol{\xi}) &= \psi_1(\xi_1)\,\psi_0(\xi_2) &&= \xi_1 \\
\Psi_2(\boldsymbol{\xi}) &= \psi_2(\xi_1)\,\psi_0(\xi_2) &&= \xi_1^2 - 1 \\
\Psi_3(\boldsymbol{\xi}) &= \psi_0(\xi_1)\,\psi_1(\xi_2) &&= \xi_2 \\
\Psi_4(\boldsymbol{\xi}) &= \psi_1(\xi_1)\,\psi_1(\xi_2) &&= \xi_1\xi_2 \\
\Psi_5(\boldsymbol{\xi}) &= \psi_2(\xi_1)\,\psi_1(\xi_2) &&= (\xi_1^2 - 1)\xi_2 \\
\Psi_6(\boldsymbol{\xi}) &= \psi_0(\xi_1)\,\psi_2(\xi_2) &&= \xi_2^2 - 1 \\
\Psi_7(\boldsymbol{\xi}) &= \psi_1(\xi_1)\,\psi_2(\xi_2) &&= \xi_1(\xi_2^2 - 1) \\
\Psi_8(\boldsymbol{\xi}) &= \psi_2(\xi_1)\,\psi_2(\xi_2) &&= (\xi_1^2 - 1)(\xi_2^2 - 1)
\end{aligned}$$

and the total number of terms N_t is

$$N_t \;=\; 1 + P \;=\; \prod_{i=1}^{n} (p_i + 1) \tag{3.10}$$

where p_i is the polynomial order bound for the i-th dimension.

It is apparent from Eq. 3.10 that the tensor-product expansion readily supports anisotropy in polynomial order for each dimension, since the polynomial order bounds for each dimension can be specified independently. It is also feasible to support anisotropy with total-order expansions, although this involves pruning polynomials that satisfy the total-order bound (potentially defined from the maximum of the per-dimension bounds) but which violate individual per-dimension bounds. In this case, Eq. 3.9 does not apply.

Additional expansion form alternatives can also be considered. Of particular interest is the tailoring of expansion form to target specific monomial coverage as motivated by the integration process employed for evaluating chaos coefficients. If the specific monomial set that can be resolved by a particular integration approach is known or can be approximated, then the chaos expansion can be tailored to synchonize with this set. Tensor-product and total-order expansions can be seen as special cases of this

general approach (corresponding to tensor-product quadrature and Smolyak sparse grids with linear growth rules, respectively), whereas, for example, Smolyak sparse grids with nonlinear growth rules could generate synchonized expansion forms that are neither tensor-product nor total-order (to be discussed later in association with Figure 3.4). In all cases, the specifics of the expansion are codified in the multi-index, and subsequent machinery for estimating response values at particular $\boldsymbol{\xi}$, evaluating response statistics by integrating over $\boldsymbol{\xi}$, etc., can be performed in a manner that is agnostic to the exact expansion formulation.

3.2.1.2 Dimension independence

A generalized polynomial basis is generated by selecting the univariate basis that is most optimal for each random input and then applying the products as defined by the multi-index to define a mixed set of multivariate polynomials. Similarly, multivariate weighting functions involve a product of the one-dimensional weighting functions and multivariate quadrature rules involve tensor products of the one-dimensional quadrature rules.

The use of independent standard random variables is the critical component that allows decoupling of the multidimensional integrals in a mixed basis expansion. It is assumed in this work that the uncorrelated standard random variables resulting from the transformation described in Section 3.2.3 can be treated as independent. This assumption is valid for uncorrelated standard normal variables (which motivates an approach of using a strictly Hermite basis for problems with correlated inputs), but could introduce significant error for other uncorrelated random variable types. For independent variables, the multidimensional integrals involved in the inner products of multivariate polynomials decouple to a product of one-dimensional integrals involving only the particular polynomial basis and corresponding weight function selected for each random dimension. The multidimensional inner products are nonzero only if each of the one-dimensional inner products is nonzero, which preserves the desired multivariate orthogonality properties for the case of a mixed basis.

3.2.2 Stochastic Collocation

The SC expansion is formed as a sum of a set of multidimensional Lagrange interpolation polynomials, one polynomial per collocation point. Since these polynomials have the feature of being equal to 1 at their particular collocation point and 0 at all other points, the coefficients of the expansion are just the response values at each of the collocation points. This can be written as:

$$R \cong \sum_{j=1}^{N_p} r_j \boldsymbol{L}_j(\boldsymbol{\xi}) \tag{3.11}$$

where the set of N_p collocation points involves a structured multidimensional grid. There is no need for tailoring of the expansion form as there is for PCE (see Section 3.2.1.1) since the polynomials that appear in the expansion are determined by the Lagrange construction (Eq. 3.1). That is, any tailoring or refinement of the expansion occurs through the selection of points in the interpolation grid and the polynomial orders of the basis adapt automatically.

As mentioned in Section 1.1, the key to maximizing performance with this approach is to use the same Gauss points defined from the optimal orthogonal polynomials as the collocation points (using either a tensor product grid as shown in Eq. 3.3 or a sum of tensor products defined for a sparse grid as shown later in Section 3.3.1.3). Given the observation that Gauss points of an orthogonal polynomial are its roots, one can factor a one-dimensional orthogonal polynomial of order p as follows:

$$\psi_j = c_j \prod_{k=1}^{p} (\xi - \xi_k) \tag{3.12}$$

where ξ_k represent the roots. This factorization is very similar to Lagrange interpolation using Gauss points as shown in Eq. 3.1. However, to obtain a Lagrange interpolant of order p from Eq. 3.1 for each of the collocation points, one must use the roots of a polynomial that is one order higher (order $p+1$) and then exclude the Gauss point being interpolated. As discussed later in Section 3.3.1.2, one also uses these higher order $p+1$ roots to evaluate the PCE coefficient integrals for expansions of order p. Thus, the collocation points used for integration or interpolation for expansions of order p are the same; however, the polynomial bases for PCE (scaled polynomial product involving all p roots of order p) and SC (scaled polynomial product involving p root subset of order $p+1$) are closely related but not identical.

3.2.3 Transformations to uncorrelated standard variables

Polynomial chaos and stochastic collocation are expanded using polynomials that are functions of independent standard random variables $\boldsymbol{\xi}$. Thus, a key component of either approach is performing a transformation of variables from the original random variables $\boldsymbol{x}$ to independent standard random variables $\boldsymbol{\xi}$ and then applying the stochastic expansion in the transformed space. The dimension of $\boldsymbol{\xi}$ is typically chosen to correspond to the dimension of $\boldsymbol{x}$, although this is not required. In fact, the dimension of $\boldsymbol{\xi}$ should be chosen to represent the number of distinct sources of randomness in a particular problem, and if individual x_i mask multiple random inputs, then the dimension of $\boldsymbol{\xi}$ can be expanded to accommodate [20]. For simplicity, all subsequent discussion will assume a one-to-one correspondence between $\boldsymbol{\xi}$ and $\boldsymbol{x}$.

This notion of independent standard space is extended over the notion of "u-space" used in reliability methods [10, 11] in that in includes not just independent standard normals, but also independent standardized uniforms, exponentials, betas and gammas. For problems directly involving independent normal, uniform, exponential, beta,

and gamma distributions for input random variables, conversion to standard form involves a simple linear scaling transformation (to the form of the density functions in Table 3.1) and then the corresponding chaos/collocation points can be employed. For other independent distributions, one has a choice of two different approaches:

1. Numerically generate an optimal polynomial basis for each independent distribution (using Gauss-Wigert [39], discretized Stieltjes [18], Chebyshev [18], or Gramm-Schmidt [51] approaches) and employ Golub-Welsch [22] to compute the corresponding Gauss points and weights.

2. Perform a nonlinear variable transformation from a given input distribution to the most similar Askey basis and employ the Askey orthogonal polynomials and associated Gauss points/weights. For example, lognormal might employ a Hermite basis in a transformed standard normal space and loguniform, triangular, and bin-based hisotgrams might employ a Legendre basis in a transformed standard uniform space.

For correlated non-normal distributions, a third approach is currently the only acceptable option (although other options are an active research area):

3. Perform a nonlinear variable transformation from all given input distributions to uncorrelated standard normal distributions and employ strictly Hermite orthogonal polynomial bases and associated Gauss points/weights.

This third approach is performed using the Nataf transformation, which is described in more detail below.

3.2.3.1 Nataf transformation

The transformation from correlated non-normal distributions to uncorrelated standard normal distributions is denoted as $\boldsymbol{\xi} = T(\mathbf{x})$ with the reverse transformation denoted as $\mathbf{x} = T^{-1}(\boldsymbol{\xi})$. These transformations are nonlinear in general, and possible approaches include the Rosenblatt [37], Nataf [7], and Box-Cox [5] transformations. The nonlinear transformations may also be linearized, and common approaches for this include the Rackwitz-Fiessler [35] two-parameter equivalent normal and the Chen-Lind [6] and Wu-Wirsching [53] three-parameter equivalent normals. The results in this report employ the Nataf nonlinear transformation, which is suitable for the common case when marginal distributions and a correlation matrix are provided, but full joint distributions are not known[1]. The Nataf transformation occurs in the following two steps. To transform between the original correlated x-space variables

[1] If joint distributions are known, then the Rosenblatt transformation is preferred.

and correlated standard normals ("z-space"), a CDF matching condition is applied for each of the marginal distributions:

$$\Phi(z_i) = F(x_i) \tag{3.13}$$

where $\Phi()$ is the standard normal cumulative distribution function and $F()$ is the cumulative distribution function of the original probability distribution. Then, to transform between correlated z-space variables and uncorrelated ξ-space variables, the Cholesky factor $\mathbf{L}$ of a modified correlation matrix is used:

$$\mathbf{z} = \mathbf{L}\boldsymbol{\xi} \tag{3.14}$$

where the original correlation matrix for non-normals in x-space has been modified to represent the corresponding "warped" correlation in z-space [7].

3.3 Non-intrusive methods for expansion formation

The major practical difference between PCE and SC is that, in PCE, one must estimate the coefficients for known basis functions, whereas in SC, one must form the interpolants for known coefficients. PCE estimates its coefficients using any of the approaches to follow: random sampling, tensor-product quadrature, Smolyak sparse grids, or linear regression. In SC, the multidimensional interpolants need to be formed over structured data sets, such as point sets from quadrature or sparse grids; approaches based on random sampling may not be used.

3.3.1 Spectral projection

The spectral projection approach projects the response against each basis function using inner products and employs the polynomial orthogonality properties to extract each coefficient. Similar to a Galerkin projection, the residual error from the approximation is rendered orthogonal to the selected basis. From Eq. 3.8, it is evident that

$$\alpha_j = \frac{\langle R, \Psi_j \rangle}{\langle \Psi_j^2 \rangle} = \frac{1}{\langle \Psi_j^2 \rangle} \int_\Omega R\, \Psi_j\, \varrho(\boldsymbol{\xi})\, d\boldsymbol{\xi}, \tag{3.15}$$

where each inner product involves a multidimensional integral over the support range of the weighting function. In particular, $\Omega = \Omega_1 \otimes \cdots \otimes \Omega_n$, with possibly unbounded intervals $\Omega_j \subset \mathbb{R}$ and the tensor product form $\varrho(\boldsymbol{\xi}) = \prod_{i=1}^{n} \varrho_i(\xi_i)$ of the joint probability density (weight) function. The denominator in Eq. 3.15 is the norm squared of the multivariate orthogonal polynomial, which can be computed analytically using the product of univariate norms squared

$$\langle \Psi_j^2 \rangle = \prod_{i=1}^{n} \langle \psi_{m_i^j}^2 \rangle \tag{3.16}$$

where the univariate inner products have simple closed form expressions for each polynomial in the Askey scheme [1]. Thus, the primary computational effort resides in evaluating the numerator, which is evaluated numerically using sampling, quadrature or sparse grid approaches (and this numerical approximation leads to use of the term "pseudo-spectral" by some investigators).

3.3.1.1 Sampling

In the sampling approach, the integral evaluation is equivalent to computing the expectation (mean) of the response-basis function product (the numerator in Eq. 3.15) for each term in the expansion when sampling within the density of the weighting function. This approach is only valid for PCE and since sampling does not provide any particular monomial coverage guarantee, it is common to combine this coefficient estimation approach with a total-order chaos expansion.

In computational practice, coefficient estimations based on sampling benefit from first estimating the response mean (the first PCE coefficient) and then removing the mean from the expectation evaluations for all subsequent coefficients [20]. While this has no effect for quadrature/sparse grid methods (see following two sections) and little effect for fully-resolved sampling, it does have a small but noticeable beneficial effect for under-resolved sampling.

3.3.1.2 Tensor product quadrature

In quadrature-based approaches, the simplest general technique for approximating multidimensional integrals, as in Eq. 3.15, is to employ a tensor product of one-dimensional quadrature rules. In the case where Ω is a hypercube, i.e. $\Omega = [-1, 1]^n$, there are several choices of nested abscissas, included Clenshaw-Curtis, Gauss-Patterson, etc. [34, 33, 19]. However, in the tensor-product case, we choose Gaussian abscissas, i.e. the zeros of polynomials that are orthogonal with respect to a density function weighting, e.g. Gauss-Hermite, Gauss-Legendre, Gauss-Laguerre, generalized Gauss-Laguerre, and Gauss-Jacobi.

We first introduce an index $i \in \mathbb{N}_+$, $i \geq 1$. Then, for each value of i, let $\{\xi_1^i, \ldots, \xi_{m_i}^i\} \subset \Omega_i$ be a sequence of abscissas for quadrature on Ω_i. For $f \in C^0(\Omega_i)$ and $n = 1$ we introduce a sequence of one-dimensional quadrature operators

$$\mathcal{U}^i(f)(\xi) = \sum_{j=1}^{m_i} f(\xi_j^i)\, w_j^i, \tag{3.17}$$

with $m_i \in \mathbb{N}$ given. When utilizing Gaussian quadrature, Eq. 3.17 integrates exactly all polynomials of degree less than or equal to $2m_i - 1$, for each $i = 1, \ldots, n$. Given an expansion order p, the highest order coefficient evaluations (Eq. 3.15) can be assumed

to involve integrands of at least polynomial order $2p$ (Ψ of order p and R modeled to order p) in each dimension such that a minimal Gaussian quadrature order of $p+1$ will be required to obtain good accuracy in these coefficients.

Now, in the multivariate case $n > 1$, for each $f \in C^0(\Omega)$ and the multi-index $\mathbf{i} = (i_1, \ldots, i_n) \in \mathbb{N}_+^n$ we define the full tensor product quadrature formulas

$$\mathcal{Q}_{\mathbf{i}}^n f(\xi) = \left(\mathcal{U}^{i_1} \otimes \cdots \otimes \mathcal{U}^{i_n}\right)(f)(\boldsymbol{\xi}) = \sum_{j_1=1}^{m_{i_1}} \cdots \sum_{j_n=1}^{m_{i_n}} f\left(\xi_{j_1}^{i_1}, \ldots, \xi_{j_n}^{i_n}\right)\left(w_{j_1}^{i_1} \otimes \cdots \otimes w_{j_n}^{i_n}\right). \tag{3.18}$$

Clearly, the above product needs $\prod_{j=1}^n m_{i_j}$ function evaluations. Therefore, when the number of input random variables is small, full tensor-product quadrature is a very effective numerical tool. On the other hand, approximations based on tensor-product grids suffer from the *curse of dimensionality* since the number of collocation points in a tensor grid grows exponentially fast in the number of input random variables. For example, if Eq. 3.18 employs the same order for all random dimensions, $m_{i_j} = m$, then Eq. 3.18 requires m^n function evaluations.

Figure 3.2 displays the monomial coverage for an integrand evaluated using an isotropic Gaussian quadrature rules in two dimensions ($m_1 = m_2 = 5$). Given this type of coverage, the traditional approach of exploying a total-order chaos expansion (involving integrands indicated by the red horizontal line) neglects a significant portion of the monomial coverage and one would expect a tensor-product expansion to provide improved synchronization and more effective usage of the Gauss point evaluations. Note that the integrand monomial coverage must resolve $2p$, such that $p_1 = p_2 = 4$ would be selected in this case.

3.3.1.3 Smolyak sparse grids

If the number of random variables is moderately large, one should rather consider sparse tensor product spaces as first proposed by Smolyak [40] and further investigated by [19, 3, 16, 54, 34, 33] that reduce dramatically the number of collocation points, while preserving a high level of accuracy.

Here we follow the notation and extend the description in [34] to describe the Smolyak *isotropic* formulas $\mathcal{A}(\mathrm{w}, n)$, where w is a level that is independent of dimension[2]. The Smolyak formulas are just linear combinations of the product formulas in Eq. 3.18 with the following key property: only products with a relatively small number of points are used. With $\mathcal{U}^0 = 0$ and for $i \geq 1$ define

$$\Delta^i = \mathcal{U}^i - \mathcal{U}^{i-1}. \tag{3.19}$$

[2]Other common formulations use a dimension-dependent level q where $q \geq n$. We use $\mathrm{w} = q - n$, where $\mathrm{w} \geq 0$ for all n.

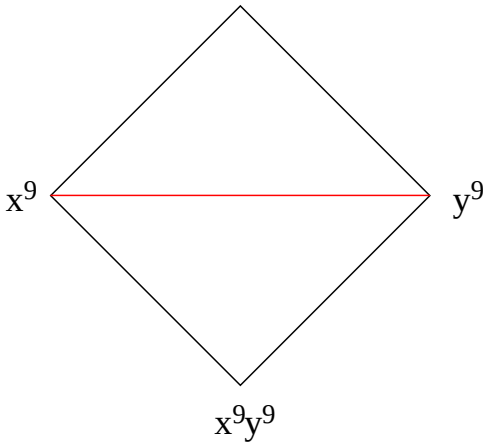

Figure 3.2. Pascal's triangle depiction of integrand monomial coverage for two dimensions and Gaussian tensor-product quadrature order = 5. Red line depicts maximal total-order integrand coverage.

and we set $|\mathbf{i}| = i_1 + \cdots + i_n$. Then the isotropic Smolyak quadrature formula is given by

$$\mathcal{A}(\mathrm{w}, n) = \sum_{|\mathbf{i}| \leq \mathrm{w}+n} \left(\Delta^{i_1} \otimes \cdots \otimes \Delta^{i_n} \right). \tag{3.20}$$

Equivalently, formula Eq. 3.20 can be written as [49]

$$\mathcal{A}(\mathrm{w}, n) = \sum_{\mathrm{w}+1 \leq |\mathbf{i}| \leq \mathrm{w}+n} (-1)^{\mathrm{w}+n-|\mathbf{i}|} \binom{n-1}{\mathrm{w}+n-|\mathbf{i}|} \cdot \left(\mathcal{U}^{i_1} \otimes \cdots \otimes \mathcal{U}^{i_n} \right). \tag{3.21}$$

Given an index set of levels, linear or nonlinear growth rules may be defined for the one-dimensional quadrature orders in order to take advantage of nesting of collocation points. The following growth rules are currently available for indices $i \geq 1$:

$$\text{Clenshaw} - \text{Curtis}: \quad m = \begin{cases} 1 & i = 1 \\ 2^{i-1} + 1 & i > 1 \end{cases} \tag{3.22}$$

$$\text{Gaussian nonlinear}: \quad m = 2^i - 1 \tag{3.23}$$

$$\text{Gaussian linear}: \quad m = 2i - 1 \tag{3.24}$$

For fully nested quadrature rules such as Clenshaw-Curtis and Gauss-Patterson, nonlinear growth rules are strongly preferred (Eq. 3.22 for the former and Eq. 3.23 for the latter). For at most weakly nested Gaussian quadrature rules, either linear or nonlinear rules may be selected, with the former motivated by finer granularity of control and uniform integrand coverage and the latter motivated by consistency with

Clenshaw-Curtis and Gauss-Patterson. The $m = 2i - 1$ linear rule takes advantage of weak nesting (e.g., Gauss-Hermite and Gauss-Legendre), whereas non-nested rules (e.g., Gauss-Laguerre) could alternatively employ an $m = i$ linear rule without any loss of reuse. In the experiments to follow, Clenshaw-Curtis employs nonlinear growth via Eq. 3.22, and all Gaussian rules employ either nonlinear growth from Eq. 3.23 or linear growth from Eq. 3.24.

Examples of isotropic sparse grids, constructed from the fully nested Clenshaw-Curtis abscissas and the weakly-nested Gaussian abscissas are shown in Figure 3.3, where $\Omega = [-1, 1]^2$. There, we consider a two-dimensional parameter space and a maximum level w = 5 (sparse grid $\mathcal{A}(5, 2)$). To see the reduction in function evaluations with respect to full tensor product grids, we also include a plot of the corresponding Clenshaw-Curtis isotropic full tensor grid having the same maximum number of points in each direction, namely $2^5 + 1 = 33$. Whereas an isotropic tensor-product quadrature scales as m^n, an isotropic sparse grid scales as $m^{\log\, n}$, significantly mitigating the curse of dimensionality.

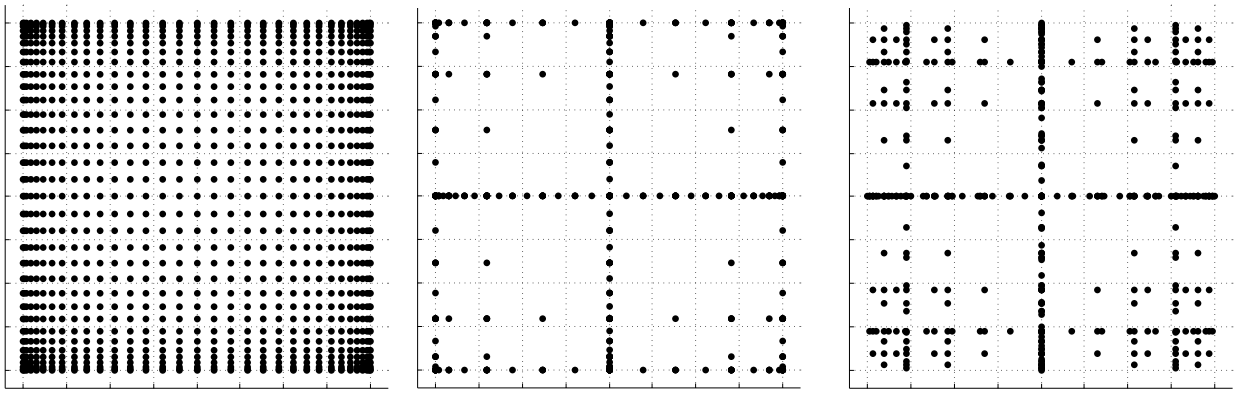

Figure 3.3. For a two-dimensional parameter space ($n = 2$) and maximum level w = 5, we plot the full tensor product grid using the Clenshaw-Curtis abscissas (left) and isotropic Smolyak sparse grids $\mathcal{A}(5, 2)$, utilizing the Clenshaw-Curtis abscissas (middle) and the Gaussian abscissas (right).

Figure 3.4 displays the monomial coverage in Pascal's triangle for an isotropic sparse grid with level $w = 4$ employing Gaussian integration rules in two dimensions. Given this geometric interpretation, subtracted tensor-product grids from Eqs. 3.20 and 3.21 can be interpreted as regions of overlap where only a single contribution to the integral should be retained. Figure 3.4(a) shows the case of nonlinear growth rules as given in Eq. 3.23 and Figure 3.4(b) shows the linear growth rule given in Eq. 3.24. Given this type of coverage, the traditional approach of exploying a total-order chaos expansion (maximal resolvable total-order integrand depicted with red

horizontal line) can be seen to be well synchronized for the case of linear growth rules, since only a few small "teeth" protrude beyond the maximal total-order basis, and to be somewhat conservative for nonlinear growth rules, since the maximal total-order basis is dictated by the concave interior and neglects the outer "legs." However, the inclusion of additional terms beyond the total-order basis in the nonlinear growth rule case, as motivated by the legs in Figure 3.4(a), is error-prone, since the order of the unknown response function will tend to push the product integrand out into the concave interior, resulting in product polynomials that are not resolvable by the sparse integration. For the total-order basis, the integrand monomial coverage must resolve $2p$, such that $p = 9$ would be selected in the nonlinear growth rule case and $p = 7$ would be selected in the linear growth rule case.

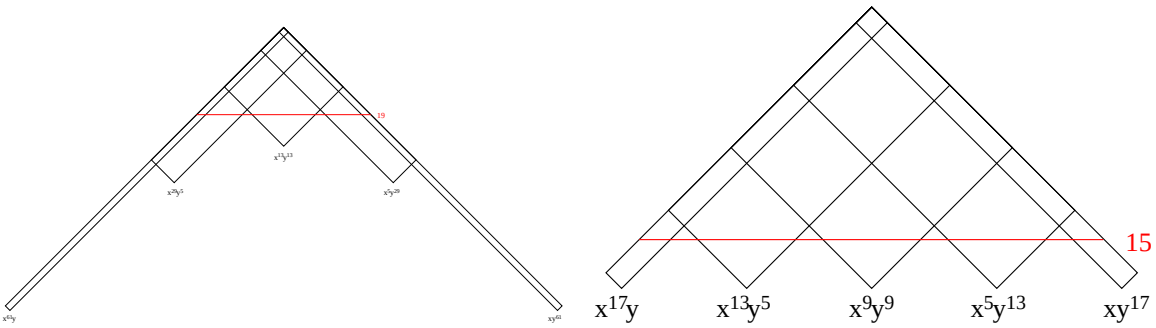

(a) Nonlinear growth rule.

(b) Linear growth rule.

Figure 3.4. Pascal's triangle depiction of integrand monomial coverage for two dimensions and Gaussian sparse grid level = 4. Red line depicts maximal total-order integrand coverage.

3.3.2 Linear regression

The linear regression approach (also known as point collocation or stochastic response surfaces [48, 26]) uses a single linear least squares solution of the form:

$$\boldsymbol{\Psi\alpha} = \boldsymbol{R} \tag{3.25}$$

to solve for the complete set of PCE coefficients $\boldsymbol{\alpha}$ that best match a set of response values $\boldsymbol{R}$. The set of response values is typically obtained by performing a design of computer experiments within the density function of $\boldsymbol{\xi}$, where each row of the matrix $\boldsymbol{\Psi}$ contains the N_t multivariate polynomial terms Ψ_j evaluated at a particular $\boldsymbol{\xi}$ sample. An over-sampling is generally advisable ([26] recommends $2N_t$ samples), resulting in a least squares solution for the over-determined system. In the case of $2N_t$ oversampling, the simulation requirements for this approach scale as $\frac{2(n+p)!}{n!p!}$,

which can be significantly more affordable than isotropic tensor-product quadrature (e.g., $(p+1)^n$) for larger problems. As for sampling-based coefficient estimation, this approach is only valid for PCE and does not provide any particular monomial coverage guarantee; thus it is common to combine this coefficient estimation approach with a total-order chaos expansion.

A closely related technique is known as the "probabilistic collocation" approach. Rather than employing random over-sampling, this technique uses a selected subset of N_t Gaussian quadrature points (those with highest tensor-product weighting), which provides more optimal collocation locations and preserves interpolation properties.

Finally, additional regression equations can be obtained through the use of derivative information (gradients and Hessians) from each collocation point, which aids greatly in scaling with respect to the number of random variables.

3.4 Nonprobabilistic Extensions to Stochastic Expansions

Stochastic expansion methods have a number of convenient analytic features that make them attractive for use within higher level analyses, such as local and global sensitivity analysis, mixed aleatory/epistemic uncertainty quantification, and design under uncertainty algorithms. First, moments of the response expansion are available analytically. Second, the response expansions are readily differentiated with respect to the underlying expansion variables, and response moment expressions may additionally be differentiated with respect to auxilliary nonprobabilistic variables.

3.4.1 Analytic moments

Mean and variance of the polynomial chaos expansion are available in simple closed form:

$$\mu_R = \langle R \rangle \cong \sum_{j=0}^{P} \alpha_j \langle \Psi_j(\boldsymbol{\xi}) \rangle = \alpha_0 \tag{3.26}$$

$$\begin{aligned} \sigma_R^2 &= \langle (R-\mu_R)^2 \rangle \cong \langle (\sum_{j=1}^{P} \alpha_j \Psi_j(\boldsymbol{\xi}))^2 \rangle = \sum_{j=1}^{P} \sum_{k=1}^{P} \alpha_j \alpha_k \langle \Psi_j(\boldsymbol{\xi}) \Psi_k(\boldsymbol{\xi}) \rangle \\ &= \sum_{j=1}^{P} \alpha_j^2 \langle \Psi_j^2 \rangle \end{aligned} \tag{3.27}$$

where the norm squared of each multivariate polynomial is computed from Eq. 3.16. The moments μ_R and σ_R are exact moments of the expansion, which converge to moments of the true response function. Higher moments are also available analytically and could be employed in moment fitting approaches (i.e., Pearson and Johnson models) in order to approximate a response PDF, although this is outside the scope of the current work.

Similar expressions can be derived for stochastic collocation:

$$\mu_R = \langle R \rangle \cong \sum_{j=1}^{N_p} r_j \langle \boldsymbol{L}_j(\boldsymbol{\xi}) \rangle = \sum_{j=1}^{N_p} r_j w_j \tag{3.28}$$

$$\begin{aligned} \sigma_R^2 &= \langle R^2 \rangle - \mu_R^2 \cong \sum_{j=1}^{N_p} \sum_{k=1}^{N_p} r_j r_k \langle \boldsymbol{L}_j(\boldsymbol{\xi}) \boldsymbol{L}_k(\boldsymbol{\xi}) \rangle - \mu_R^2 \\ &= \sum_{j=1}^{N_p} r_j^2 w_j - \mu_R^2 \end{aligned} \tag{3.29}$$

where the expectation of a particular Lagrange polynomial constructed at Gauss points and then integrated at these same Gauss points leaves only the weight corresponding to the point for which the interpolation value is one.

3.4.2 Stochastic Sensitivity Analysis

3.4.2.1 Global sensitivity analysis: interpretation of PCE coefficients

In the case of PCE, the chaos coefficients provide information on the global sensitivity of the response with respect to the expansion variables. As described in [42], variance-based decomposition (VBD) has much in common with expansions based on orthogonal polynomial bases, and it is straighforward to analytically compute Sobol' sensitivity indices from the set of PCE coefficients as a post-processing step. This allows an assessment of which expansion variables are most influential in contributing to the output uncertainty. Recent work [46] has extended this to SC expansions and demonstrated improved performance of PCE/SC sensitivity analysis approaches relative to VBD using sampling methods.

3.4.2.2 Local sensitivity analysis: derivatives with respect to expansion variables

Polynomial chaos expansions are easily differentiated with respect to the random variables [36]. First, using Eq. 3.8,

$$\frac{dR}{d\xi_i} \cong \sum_{j=0}^{P} \alpha_j \frac{d\Psi_j(\boldsymbol{\xi})}{d\xi_i} \tag{3.30}$$

and then using Eq. 3.7,

$$\frac{d\Psi_j(\boldsymbol{\xi})}{d\xi_i} = \frac{d\psi_i}{d\xi_i} \prod_{\substack{k=1 \\ k \neq i}}^{n} \psi_{m_k^j}(\xi_k) \tag{3.31}$$

where the univariate polynomial derivatives $\frac{d\psi_i}{d\xi_i}$ have simple closed form expressions for each polynomial in the Askey scheme [1]. Finally, using the Jacobian of the Nataf variable transformation,

$$\frac{dR}{dx_i} = \frac{dR}{d\boldsymbol{\xi}} \frac{d\boldsymbol{\xi}}{dx_i} \tag{3.32}$$

which simplifies to $\frac{dR}{d\xi_i} \frac{d\xi_i}{dx_i}$ in the case of uncorrelated x_i.

Similar expressions may be derived for stochastic collocation, starting from Eq. 3.11:

$$\frac{dR}{d\xi_i} = \sum_{j=1}^{N_p} r_j \frac{d\boldsymbol{L}_j(\boldsymbol{\xi})}{d\xi_i} \tag{3.33}$$

where the multidimensional interpolant $\boldsymbol{L}_j$ is formed over either tensor-product quadrature points or a Smolyak sparse grid. For the former case, the derivative of the multidimensional interpolant $\boldsymbol{L}_j$ involves a product rule of the one-dimensional interpolants L_k:

$$\frac{d\boldsymbol{L}_j(\boldsymbol{\xi})}{d\xi_i} = \frac{dL_i}{d\xi_i} \prod_{\substack{k=1 \\ k \neq i}}^{n} L_k(\xi_k) \tag{3.34}$$

and for the latter case, the derivative involves a linear combination of these product rules, as dictated by the Smolyak recursion shown in Eq. 3.21. Finally, calculation of $\frac{dR}{dx_i}$ involves the same Jacobian application shown in Eq. 3.32.

3.4.2.3 Local sensitivity analysis: derivatives of probabilistic expansions with respect to nonprobabilistic variables

With the introduction of nonprobabilistic variables $\boldsymbol{s}$ (for example, design variables or epistemic uncertain variables), a polynomial chaos expansion only over the random

variables $\boldsymbol{\xi}$ has the functional relationship:

$$R(\boldsymbol{\xi}, \boldsymbol{s}) \cong \sum_{j=0}^{P} \alpha_j(\boldsymbol{s}) \Psi_j(\boldsymbol{\xi}) \tag{3.35}$$

In this case, sensitivities of the mean and variance in Eqs. 3.26 and 3.27 with respect to the nonprobabilistic variables are as follows:

$$\frac{d\mu_R}{ds} = \frac{d\alpha_0}{ds} = \frac{d}{ds}\langle R \rangle = \langle \frac{dR}{ds} \rangle \tag{3.36}$$

$$\frac{d\sigma_R^2}{ds} = \sum_{j=1}^{P} \langle \Psi_j^2 \rangle \frac{d\alpha_j^2}{ds} = 2 \sum_{j=1}^{P} \alpha_j \langle \frac{dR}{ds}, \Psi_j \rangle \tag{3.37}$$

since

$$\frac{d\alpha_j}{ds} = \frac{\langle \frac{dR}{ds}, \Psi_j \rangle}{\langle \Psi_j^2 \rangle} \tag{3.38}$$

The coefficients calculated in Eq. 3.38 may be interpreted as either the nonprobabilistic sensitivities of the chaos coefficients for the response expansion or the chaos coefficients of an expansion for the nonprobabilistic sensitivities of the response. The evaluation of integrals involving $\frac{dR}{ds}$ extends the data requirements for the PCE approach to include response sensitivities at each of the sampling points for the quadrature, sparse grid, sampling, or point collocation coefficient estimation approaches. The resulting expansions are valid only for a particular set of nonprobabilistic variables and must be recalculated each time the nonprobabilistic variables are modified.

Similarly for stochastic collocation,

$$R(\boldsymbol{\xi}, \boldsymbol{s}) \cong \sum_{j=1}^{N_p} r_j(\boldsymbol{s}) \boldsymbol{L}_j(\boldsymbol{\xi}) \tag{3.39}$$

leads to

$$\frac{d\mu_R}{ds} = \frac{d}{ds}\langle R \rangle = \sum_{j=1}^{N_p} \frac{dr_j}{ds} \langle \boldsymbol{L}_j \rangle = \sum_{j=1}^{N_p} w_j \frac{dr_j}{ds} \tag{3.40}$$

$$\frac{d\sigma_R^2}{ds} = \sum_{j=1}^{N_p} 2 w_j r_j \frac{dr_j}{ds} - 2\mu_R \frac{d\mu_R}{ds} = \sum_{j=1}^{N_p} 2 w_j (r_j - \mu_R) \frac{dr_j}{ds} \tag{3.41}$$

based on differentiation of Eqs. 3.28-3.29.

3.4.2.4 Local sensitivity analysis: derivatives of combined expansions with respect to nonprobabilistic variables

Alternatively, a stochastic expansion can be formed over both $\boldsymbol{\xi}$ and $\boldsymbol{s}$. Assuming a bounded domain $\boldsymbol{s}_L \leq \boldsymbol{s} \leq \boldsymbol{s}_U$ (with no implied probability content) for the nonprobabilistic variables, a Legendre chaos basis would be appropriate for each of the dimensions in $\boldsymbol{s}$ within a polynomial chaos expansion.

$$R(\boldsymbol{\xi}, \boldsymbol{s}) \cong \sum_{j=0}^{P} \alpha_j \Psi_j(\boldsymbol{\xi}, \boldsymbol{s}) \tag{3.42}$$

In this case, sensitivities for the mean and variance do not require response sensitivity data, but this comes at the cost of forming the PCE over additional dimensions. For this combined variable expansion, the mean and variance are evaluated by performing the expectations over only the probabilistic expansion variables, which eliminates the polynomial dependence on $\boldsymbol{\xi}$, leaving behind the desired polynomial dependence of the moments on $\boldsymbol{s}$:

$$\mu_R(\boldsymbol{s}) = \sum_{j=0}^{P} \alpha_j \langle \Psi_j(\boldsymbol{\xi}, \boldsymbol{s}) \rangle_{\boldsymbol{\xi}} \tag{3.43}$$

$$\sigma_R^2(\boldsymbol{s}) = \sum_{j=0}^{P} \sum_{k=0}^{P} \alpha_j \alpha_k \langle \Psi_j(\boldsymbol{\xi}, \boldsymbol{s}) \Psi_k(\boldsymbol{\xi}, \boldsymbol{s}) \rangle_{\boldsymbol{\xi}} - \mu_R^2(\boldsymbol{s}) \tag{3.44}$$

The remaining polynomials may then be differentiated with respect to $\boldsymbol{s}$. In this approach, the combined PCE is valid for the full nonprobabilistic variable range ($\boldsymbol{s}_L \leq \boldsymbol{s} \leq \boldsymbol{s}_U$) and does not need to be updated for each change in nonprobabilistic variables, although adaptive localization techniques (i.e., trust region model management approaches) can be employed when improved local accuracy of the sensitivities is required.

Similarly for stochastic collocation,

$$R(\boldsymbol{\xi}, \boldsymbol{s}) \cong \sum_{j=1}^{N_p} r_j \boldsymbol{L}_j(\boldsymbol{\xi}, \boldsymbol{s}) \tag{3.45}$$

leads to

$$\mu_R(\boldsymbol{s}) = \sum_{j=1}^{N_p} r_j \langle \boldsymbol{L}_j(\boldsymbol{\xi}, \boldsymbol{s}) \rangle_{\boldsymbol{\xi}} \tag{3.46}$$

$$\sigma_R^2(\boldsymbol{s}) = \sum_{j=1}^{N_p} \sum_{k=1}^{N_p} r_j r_k \langle \boldsymbol{L}_j(\boldsymbol{\xi}, \boldsymbol{s}) \boldsymbol{L}_k(\boldsymbol{\xi}, \boldsymbol{s}) \rangle_{\boldsymbol{\xi}} - \mu_R^2(\boldsymbol{s}) \tag{3.47}$$

where the remaining polynomials not eliminated by the expectation over $\boldsymbol{\xi}$ are again differentiated with respect to $\boldsymbol{s}$.

3.4.2.5 Inputs and outputs

There are two types of nonprobabilistic variables for which sensitivities must be calculated: "augmented," where the nonprobabilistic variables are separate from and augment the probabilistic variables, and "inserted," where the nonprobabilistic variables define distribution parameters for the probabilistic variables. While one could artificially augment the dimensionality of a combined variable expansion approach with inserted nonprobabilistic variables, this is not currently explored in this work. Thus, any inserted nonprobabilistic variable sensitivities must be handled using Eqs. 3.36-3.37 and Eqs. 3.40-3.41 where $\frac{dR}{ds}$ is calculated as $\frac{dR}{dx}\frac{dx}{ds}$ and $\frac{dx}{ds}$ is the Jacobian of the variable transformation $\mathbf{x} = T^{-1}(\boldsymbol{\xi})$ with respect to the inserted nonprobabilistic variables.

While moment sensitivities directly enable robust design optimization formulations which seek to control response variance, design for reliability requires design sensitivities of tail statistics. In this work, we initially focus on design sensitivity of simple moment projections for this purpose. In reliability analysis using the Mean Value method, forward ($\bar{z} \rightarrow \beta$) and inverse ($\bar{\beta} \rightarrow z$) mappings employing the reliability index are approximated as [10, 11]:

$$\beta_{cdf} = \frac{\mu_R - \bar{z}}{\sigma_R} \tag{3.48}$$

$$\beta_{ccdf} = \frac{\bar{z} - \mu_R}{\sigma_R} \tag{3.49}$$

$$z = \mu_R - \sigma_R \bar{\beta}_{cdf} \tag{3.50}$$

$$z = \mu_R + \sigma_R \bar{\beta}_{ccdf} \tag{3.51}$$

such that it is straightforward to form approximate design sensitivities of β and z from the PCE moment sensitivities. From here, approximate design sensitivities of probability levels may also be formed given a probability expression (such as $\Phi(-\beta)$) for the reliability index. The current alternative of numerical design sensitivities of sampled probability levels would employ fewer simplifying approximations, but would also be much more expensive to compute accurately and is avoided for now. Future capabilities for analytic probability sensitivities could be based on Pearson/Johnson model for analytic response PDFs or sampling sensitivity approaches.

Chapter 4

Analytic Benchmarks and Results

Capabilities for uncertainty analysis based on stochastic expansions and optimization-based interval estimation have been implemented in DAKOTA [9], an open-source software framework for design and performance analysis of computational models on high performance computers. This section examines computational performance of these algorithmic approaches for several algebraic benchmark test problems. These results build upon PCE results for UQ presented in [15], comparisons of PCE and SC results for UQ presented in [12], PCE-based and SC-based optimization under uncertainty (OUU) results presented in [14], and OUU and interval estimation results presented in [8].

4.1 Short column

This test problem involves the plastic analysis of a short column with rectangular cross section (width $b = 5$ and depth $h = 15$) having uncertain material properties (yield stress Y) and subject to uncertain loads (bending moment M and axial force P) [29]. The limit state function is defined as:

$$g(\mathbf{x}) = 1 - \frac{4M}{bh^2Y} - \frac{P^2}{b^2h^2Y^2} \tag{4.1}$$

The distributions for P, M, and Y are Normal(500, 100), Normal(2000, 400), and Lognormal(5, 0.5), respectively, with a correlation coefficient of 0.5 between P and M (uncorrelated otherwise). For P and M, a linear variable transformation is applied and Hermite orthogonal polynomials are employed in the transformed standard normal space. For Y, two polynomial approximation approaches are employed: (1) a nonlinear variable transformation is applied and Hermite orthogonal polynomials are employed in the transformed standard normal space, or (2) Gauss-Wigert orthogonal polynomials are numerically generated.

4.1.1 Uncertainty quantification with PCE and SC

Figure 4.1 shows convergence of the mean and standard deviation of the limit state function for increasing tensor-product quadrature orders, sparse grid levels using linear growth, and sparse grid levels using nonlinear growth for tailored PCE (synchronized tensor-product and total-order expansions as shown in Figures 3.2 and 3.4), traditional PCE (total-order expansions based on heuristics), and SC. Since an analytic solution is not available, residuals are measured relative to an "overkill" solution. The quality of this overkill solution and the effect of compounded round-off errors can be seen to hinder the convergence trajectories at residual values below 10^{-10} (short of double precision machine epsilon).

In Figure 4.1(a), the only discernible differences appear among the set of tensor-product quadrature (TPQ) results, the set of linear growth Smolyak sparse grids (SSG) results, and the set of nonlinear growth SSG results, with similar performance among the three sets. In Figures 4.1(b,c), however, significant differences are evident. First, for TPQ (Figure 4.1(b)), tensor-product PCE (tailored) is shown to completely eliminate the performance gap between total-order PCE (traditional) and SC. For SSG with nonlinear growth rules (Figure 4.1(c), blue lines), the heuristic total-order PCE approach (traditional) is shown to be nonconservative in its estimation of the order of expansion to employ. Through inclusion of monomials that exceed the order of what can be resolved, the expansion standard deviation fails to converge. The synchronized total-order PCE approach (tailored) is shown to be much more rigorous for nonlinear growth, although its performance falls well short of that of SC with nonlinear growth. Without this rigorous estimation, however, one would be left with the undesirable alternative of trial and error in synchronizing a nonlinear SSG with a PCE expansion order. For SSG with linear growth rules (Figure 4.1(c), green lines), improved heuristics are available and the synchronized and heuristic total-order PCE approaches can be seen to be identical. Thus, in the linear case, rigorous estimation of the set of nondominated monomials is not required. Further, while the performance gap with SC remains, its magnitude has been reduced relative to the gap in the nonlinear SSG case. Whereas TPQ outperforms linear/nonlinear SSG for two-dimensional problems shown in [12] (such that the equivalent tailored PCE and SC TPQ approaches performed the best), this trend has started to reverse with the increase to three dimensions and SC with linear SSG stands alone as the most rapidly converging technique. Finally, numerically-generated polynomial bases (Gauss-Wigert for the lognormal variable) can be seen to converge more slowly than Askey bases applied in the transformed space. This trend is fairly consistent for rational functions with lognormals in the denominator, indicating that the variable transformations reduce the overall nonlinearity (presumably from increasing the polynomial order of the denominator) in this case.

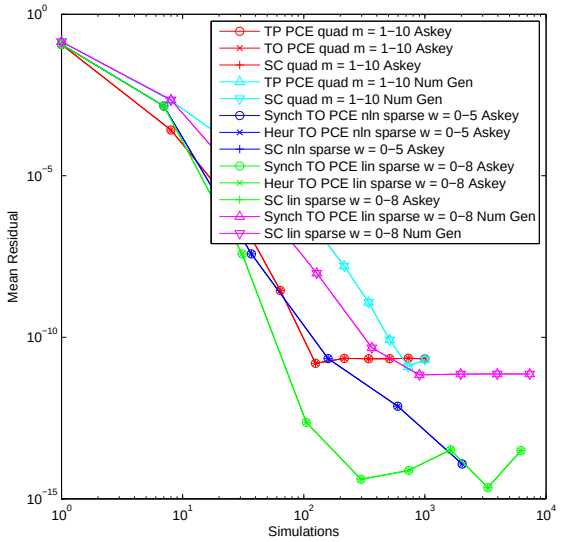

(a) Mean residual (TPQ and SSG).

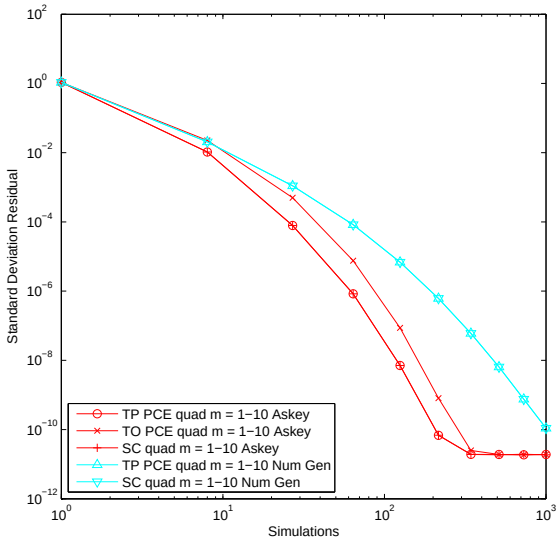

(b) Standard deviation residual (TPQ).

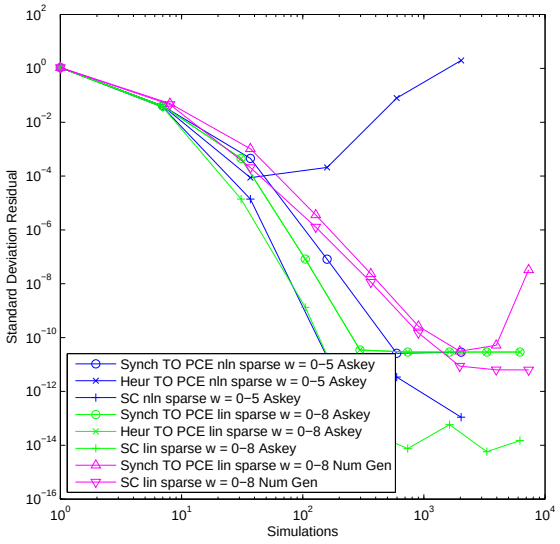

(c) Standard deviation residual (SSG).

Figure 4.1. Convergence of mean and standard deviation for the short column test problem.

Table 4.1. PCE-based and SC-based interval estimation results, short column test problem.

Interv Est Approach	UQ Approach	Expansion Variables	Evaluations (Fn, Grad)	Area	β
EGO	PCE SSG w = 1	Aleatory	(84/91, 0/0)	[75.0002, 374.999]	[-2.27098, 11.8828]
EGO	PCE SSG w = 2	Aleatory	(372/403, 0/0)	[75.0002, 374.999]	[-2.18824, 11.5924]
EGO	PCE SSG w = 3	Aleatory	(1260/1365, 0/0)	[75.0002, 374.999]	[-2.18732, 11.5900]
EGO	PCE SSG w = 4	Aleatory	(3564/3861, 0/0)	[75.0002, 374.999]	[-2.18732, 11.5900]
EGO	PCE PC p = 1	Aleatory	(96/104, 0/0)	[75.0002, 374.999]	[-2.48326, 12.3899]
EGO	PCE PC p = 2	Aleatory	(240/260, 0/0)	[75.0002, 374.999]	[-2.18786, 11.6106]
EGO	PCE PC p = 3	Aleatory	(480/520, 0/0)	[75.0002, 374.999]	[-2.18950, 11.5987]
EGO	PCE PC p = 4	Aleatory	(840/910, 0/0)	[75.0002, 374.999]	[-2.18744, 11.5905]
EGO	PCE SSG w = 4	Combined	(1341/1341, 0/0)	[75.0002, 374.999]	[-2.31709, 17.6164]
EGO	PCE SSG w = 6	Combined	(13683/13683, 0/0)	[75.0002, 374.999]	[-2.18969, 11.6939]
EGO	PCE SSG w = 8	Combined	(94473/94473, 0/0)	[75.0002, 374.999]	[-2.18734, 11.5910]
EGO	PCE PC p = 4	Combined	(252/252, 0/0)	[75.0002, 374.999]	[-2.30398, 11.4164]
EGO	PCE PC p = 6	Combined	(924/924, 0/0)	[75.0002, 374.999]	[-2.22130, 12.1568]
EGO	PCE PC p = 8	Combined	(2574/2574, 0/0)	[75.0002, 374.999]	[-2.19048, 11.6776]
EGO	SC SSG w = 1	Aleatory	(84/91, 0/0)	[75.0002, 374.999]	[-2.26264, 11.8623]
EGO	SC SSG w = 2	Aleatory	(372/403, 0/0)	[75.0002, 374.999]	[-2.18735, 11.5900]
EGO	SC SSG w = 3	Aleatory	(1260/1365, 0/0)	[75.0002, 374.999]	[-2.18732, 11.5900]
EGO	SC SSG w = 4	Aleatory	(3564/3861, 0/0)	[75.0002, 374.999]	[-2.18732, 11.5900]
EGO	SC SSG w = 4	Combined	(1341/1341, 0/0)	[75.0002, 374.999]	[-2.23439, 12.3640]
EGO	SC SSG w = 6	Combined	(13683/13683, 0/0)	[75.0002, 374.999]	[-2.18804, 11.6002]
EGO	SC SSG w = 8	Combined	(94473/94473, 0/0)	[75.0002, 374.999]	[-2.18732, 11.5901]
NPSOL	PCE SSG w = 1	Aleatory	(21/77, 21/77)	[75.0000, 375.000]	[-2.27098, 11.8829]
NPSOL	PCE SSG w = 2	Aleatory	(93/341, 93/341)	[75.0000, 375.000]	[-2.18824, 11.5924]
NPSOL	PCE SSG w = 3	Aleatory	(315/1155, 315/1155)	[75.0000, 375.000]	[-2.18732, 11.5900]
NPSOL	PCE SSG w = 4	Aleatory	(891/3267, 891/3267)	[75.0000, 375.000]	[-2.18732, 11.5900]
NPSOL	PCE SSG w = 4	Combined	(1341/1341, 0/0)	[75.0000, 375.000]	[-2.31709, 17.6167]
NPSOL	PCE SSG w = 6	Combined	(13683/13683, 0/0)	[75.0000, 375.000]	[-2.18969, 11.6940]
NPSOL	PCE SSG w = 8	Combined	(94473/94473, 0/0)	[75.0000, 375.000]	[-2.18735, 11.5911]
NPSOL	SC SSG w = 1	Aleatory	(21/77, 21/77)	[75.0000, 375.000]	[-2.26264, 11.8623]
NPSOL	SC SSG w = 2	Aleatory	(93/341, 93/341)	[75.0000, 375.000]	[-2.18735, 11.5901]
NPSOL	SC SSG w = 3	Aleatory	(315/1155, 315/1155)	[75.0000, 375.000]	[-2.18732, 11.5900]
NPSOL	SC SSG w = 4	Aleatory	(891/3267, 891/3267)	[75.0000, 375.000]	[-2.18732, 11.5900]
NPSOL	SC SSG w = 4	Combined	(1341/1341, 0/0)	[75.0000, 375.000]	[-2.23440, 12.3640]
NPSOL	SC SSG w = 6	Combined	(13683/13683, 0/0)	[75.0000, 375.000]	[-2.18804, 11.6003]
NPSOL	SC SSG w = 8	Combined	(94473/94473, 0/0)	[75.0000, 375.000]	[-2.18733, 11.5901]
LHS 100	LHS 100	N/A	(10^4/10^4, 0/0)	[80.5075, 338.607]	[-2.14505, 8.64891]
LHS 1000	LHS 1000	N/A	(10^6/10^6, 0/0)	[76.5939, 368.225]	[-2.19883, 11.2353]
LHS 10^4	LHS 10^4	N/A	(10^8/10^8, 0/0)	[76.4755, 373.935]	[-2.16323, 11.5593]

4.1.2 Epistemic interval estimation

As for the optimization under uncertainty problem described in [14], we will study the cross-sectional area bh and reliability index β. However, rather than optimizing the area subject to a constraint on the reliability index, we will determine the output interval in these metrics resulting from epistemic uncertainties, where the epistemic variables are taken to be the beam width b and depth h (previously the design variables) with intervals of [5.0, 15.] and [15., 25.], respectively. The interval optimizer is either the nongradient-based EGO algorithm, based on successive refinement of Gaussian process surrogate models, or the gradient-based NPSOL algorithm, employing stochastic sensitivities. Smolyak sparse grids (SSG) with linear growth rules are employed for tailored total-order PCE and SC with aleatory and combined expansions, and point collocation (PC) is employed for total-order PCE with an oversampling ratio of two.

Table 4.1 shows the results for a convergence study with increasing SSG levels for PCE and SC and increasing PC expansion orders for PCE compared to nested Latin hypercube sampling. It is evident that the PCE/SC aleatory expansion results using SSG converge by w = 3 (highlighted in red) with an area interval of $[75., 375.]$ and a β interval of $[-2.18732, 11.5900]$. The PCE/SC combined expansion results using SSG

also converge, although more slowly; by w = 8 (highlighted in green), the PCE results are accurate only to four digits and the SC results are only accurate to five digits. SC consistently outperforms PCE for this problem and numerical integration (SSG) generally provides more accurate results than regression (PC), such that the SC SSG aleatory expansion approach is the best performer, converging to five or six digits of accuracy by w = 2 at an expense of 403 limit state function evaluations for EGO and 341 limit state function and gradient evaluations for NPSOL (both highlighted in blue). Both gradient-based and nongradient-based interval optimization approaches converge to the same solution for all cases, indicating monotonicity in the aleatory metrics as a function of the epistemic parameters, and the gradient-based local approach requires fewer aleatory expansion reconstructions than the nongradient-based approach, although the gradient-based reconstructions require the addition of response derivative information. The nested sampling results are also converging to the correct intervals, although the results are only accurate to one or two digits for the area interval and two or three digits for the reliability index interval after 10^8 samples (highlighted in magenta). Comparing this result to the SC SSG aleatory expansion approach with five digits of accuracy at either 403 or 341 limit state evaluations, *our proposed approach reduces expense by greater than five orders of magnitude while achieving more precise results*. Comparable accuracy could likely have been obtained with more exhaustive nested sampling (resulting in additional orders of magnitude in computational savings when requiring comparable interval accuracy), but these computational experiments were too expensive to perform.

To investigate the issue of the degraded convergence rates for combined expansions, Figure 4.2 shows a comparison of convergence rates for L_2 versus L_∞ metrics for the short column problem, where all five variables are used in combined expansions. The L_∞ metrics are the β intervals shown previously in Table 4.1. For the L_2 case, all five variables are treated as aleatory and convergence in β value is shown[1]. It is evident that L_2 convergence rates are more rapid than L_∞, with approximately five orders of magnitude reduction in residuals for L_∞ compared to approximately ten orders of magnitude reduction in residuals for L_2. Thus, the decreased performance in combined expansions relative to aleatory expansions is due to more than the increased dimensionality; the point-wise accuracy required for L_∞ is more demanding than the weak convergence required for L_2.

4.2 Cantilever beam

The next test problem involves the simple uniform cantilever beam [43, 52] shown in Figure 4.3. Random variables in the problem include the yield stress R and Youngs modulus E of the beam material and the horizontal and vertical loads, X and Y, which

[1]Note that the different β estimates produced in these two analyses reflect different conditional expectations and one does not bound the other; rather, the point is relative convergence rates for different types of metrics.

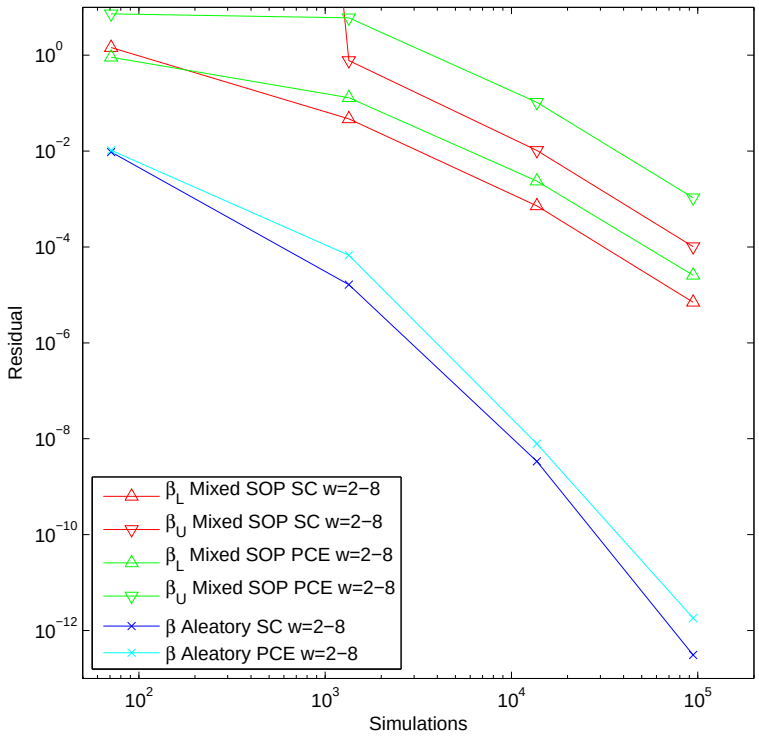

Figure 4.2. Convergence rates for combined expansions in the short column test problem.

are modeled with independent normal distributions using N(40000, 2000), N(2.9E7, 1.45E6), N(500, 100), and N(1000, 100), respectively. Problem constants include $L = 100$ in. and $D_0 = 2.2535$ in. The beam response metrics have the following analytic form:

$$\text{stress} = \frac{600}{wt^2}Y + \frac{600}{w^2t}X \leq R \tag{4.2}$$

$$\text{displacement} = \frac{4L^3}{Ewt}\sqrt{(\frac{Y}{t^2})^2 + (\frac{X}{w^2})^2} \leq D_0 \tag{4.3}$$

These stress and displacement response functions are scaled using $\frac{\text{stress}}{R} - 1$ and $\frac{\text{displacement}}{D_0} - 1$, such that negative values indicate safe regions of the parameter space. For polynomial approximation, a linear variable transformation is used to account for scaling of the normal PDFs and Hermite orthogonal polynomials are employed in the transformed standard normal space.

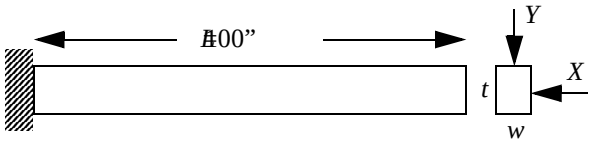

Figure 4.3. Cantilever beam test problem.

4.2.1 Uncertainty quantification with PCE and SC

Figure 4.4 shows convergence of the mean residuals and Figure 4.5 shows convergence of the standard deviation residuals for scaled stress and displacement for increasing quadrature orders and sparse grid levels using tailored PCE, traditional PCE, and SC. An analytic solution is again unavailable, so residuals are measured relative to an "overkill" solution such that convergence again slows at residual values below 10^{-10}.

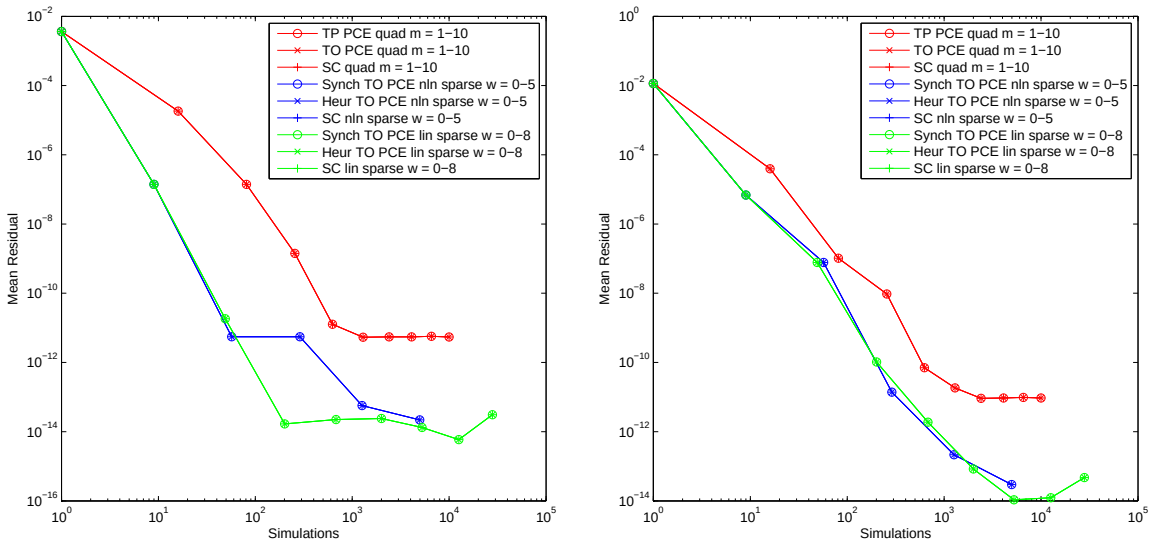

(a) Scaled stress (TPQ and SSG).

(b) Scaled displacement (TPQ and SSG).

Figure 4.4. Convergence of mean for PCE and SC in the cantilever beam test problem.

In Figure 4.4, the only discernible difference appears between the sets of TPQ, linear SSG, and nonlinear SSG results, with linear/nonlinear SSG outperforming TPQ for this four-dimensional problem. In Figure 4.5, additional differences are again evident. For TPQ (red lines), the performance gap between total-order PCE (traditional) and SC is relatively small, but tensor-product PCE (tailored) is again shown to completely eliminate it. For nonlinear SSG (blue lines), the heuristic total-order PCE approach (traditional) is again shown to be nonconservative in its estimation of the order of

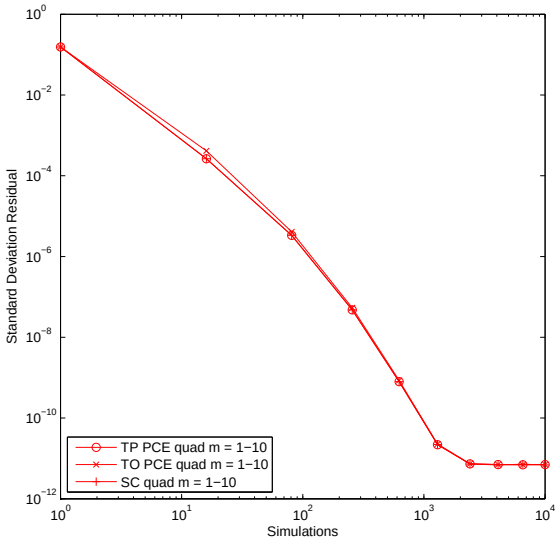

(a) Scaled stress (TPQ).

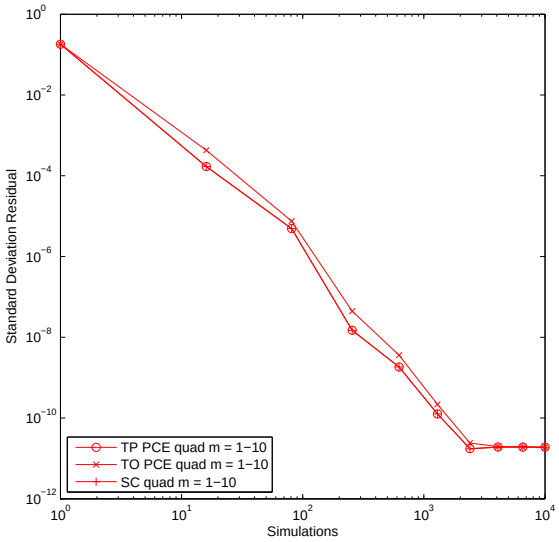

(b) Scaled displacement (TPQ).

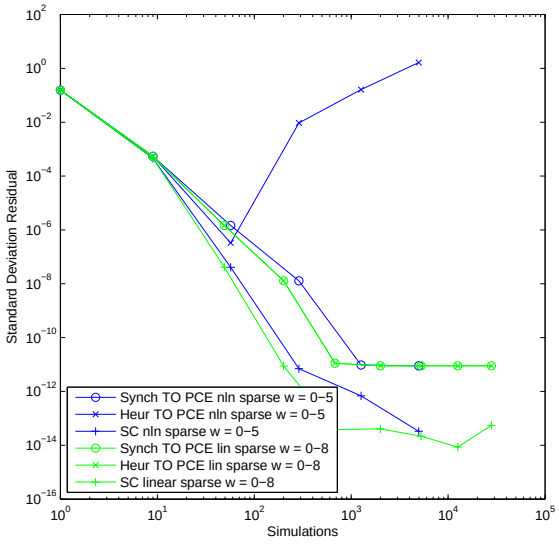

(c) Scaled stress (SSG).

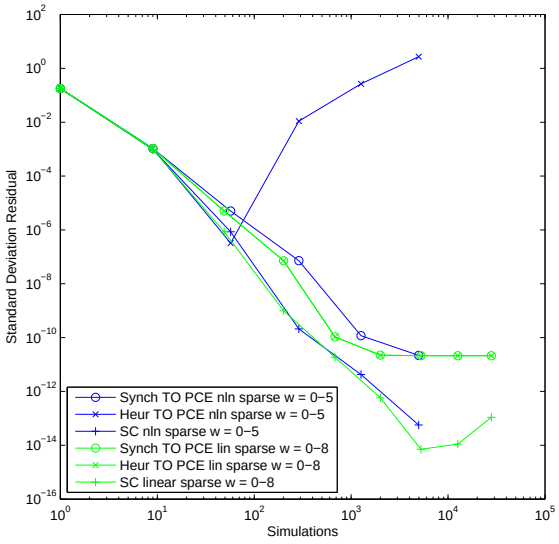

(d) Scaled displacement (SSG).

Figure 4.5. Convergence of standard deviation for PCE and SC in the cantilever beam test problem.

expansion to employ, and the synchronized total-order PCE approach (tailored) is shown to be more rigorous, although it again falls short of the performance of SC. For linear SSG (green lines), synchronized and heuristic total-order PCE approaches are again identical and, while the performance gap with SC remains, its magnitude has been reduced relative to the gap in the nonlinear SSG case. As for the previous three-dimensional problem (Figure 4.1(b)), SC with linear SSG stands alone as the most efficient technique.

4.2.2 Epistemic interval estimation

As for the optimization under uncertainty problem described in [14], we will study the cross-sectional area wt and reliability indices β_S and β_D for stress and displacement, respectively. However, rather than optimizing an objective subject to constraints, we will determine the output interval in these metrics resulting from epistemic uncertainties, where the epistemic variables are taken to be the beam width w and thickness t (previously the design variables) with intervals of [1.0, 10.]. The optimizer is again either the nongradient-based EGO algorithm or the gradient-based NPSOL algorithm. Smolyak sparse grids (SSG) with linear growth rules are employed for tailored total-order PCE and SC with aleatory and combined expansions, and point collocation (PC) is employed for total-order PCE with an oversampling ratio of two.

Table 4.2 shows the results for a convergence study with increasing SSG levels for PCE and SC and increasing PC expansion orders for PCE compared to nested Latin hypercube sampling. It is evident that the PCE/SC aleatory expansion results using SSG converge by w = 3 (highlighted in red) with an area interval of $[1., 100.]$, a β_S interval of $[-8.9921, 404.96]$ and a β_D interval of $[-9.6345, 1409.6]$. While the nested sampling results are slowly converging to these intervals, accuracy is limited to at most two digits after 10^8 samples (highlighted in magenta). The PCE/SC combined expansions using SSG also appear to be slowly converging to the correct reliability index intervals, but upper bound accuracy is poor even at the highest w = 8 level (highlighted in green). In addition, the reliability index upper bounds for most of the SC combined expansions have diverged resulting from negative expansion variance (this cannot happen with PCE, but is possible for SC, particularly for sparse grids when collocation weights can be negative – see Eqs. 3.27 and 3.29). Again, the PCE PC regression-based results scale well, but accuracy lags SSG numerical integrations. In addition, the PCE PC combined expansion approach does not appear to be converging, likely due to ill-conditioning in the linear least squares solution. Overall, the SC aleatory expansion approach using SSG is the best performer, with good accuracy at w = 2 at the cost of 931 stress and 1960 displacement function evaluations for EGO or 245 stress and 147 displacement function/gradient evaluations for NPSOL (both highlighted in blue). Comparing this result to the nested sampling result, *our proposed approach is again much more efficient, reducing expense by five to six orders of magnitude, while achieving much more precise results, four to six digits of accuracy instead of zero to two.*

Table 4.2. PCE-based and SC-based interval estimation results, cantilever beam test problem.

Interv Est Approach	UQ Approach	Expansion Variables	Evaluations (Fn, Grad)	Area	β_S	β_D
EGO	PCE SSG w=1	Aleatory	(108/171/369, 0/0/0)	[1.00002, 99.9998]	[-9.02367, 406.390]	[-9.69101, 1417.85]
EGO	PCE SSG w=2	Aleatory	(588/931/1960, 0/0/0)	[1.00002, 99.9998]	[-8.99220, 404.967]	[-9.63475, 1409.61]
EGO	PCE SSG w=3	Aleatory	(2412/3819/8040, 0/0/0)	[1.00002, 99.9998]	[-8.99211, 404.963]	[-9.63448, 1409.57]
EGO	PCE SSG w=4	Aleatory	(8172/12939/27240, 0/0/0)	[1.00002, 99.9998]	[-8.99211, 404.963]	[-9.63448, 1409.57]
EGO	PCE PC p=1	Aleatory	(120/200/400, 0/0/0)	[1.00002, 99.9998]	[-9.12054, 411.796]	[-9.64808, 1413.25]
EGO	PCE PC p=2	Aleatory	(360/570/1230, 0/0/0)	[1.00002, 99.9998]	[-8.98064, 404.434]	[-9.63209, 1409.51]
EGO	PCE PC p=3	Aleatory	(840/1330/2800, 0/0/0)	[1.00002, 99.9998]	[-8.99177, 404.954]	[-9.63600, 1409.83]
EGO	PCE PC p=4	Aleatory	(1680/2660/5600, 0/0/0)	[1.00002, 99.9998]	[-8.99218, 404.965]	[-9.63455, 1409.58]
EGO	PCE SSG w=4	Combined	(2381/2381/2381, 0/0/0)	[1.00002, 99.9998]	[-12.0227, 28.4165]	[-12.8208, 13.9021]
EGO	PCE SSG w=6	Combined	(30869/30869/30869, 0/0/0)	[1.00002, 99.9998]	[-9.83782, 223.547]	[-10.9817, 60.0065]
EGO	PCE SSG w=8	Combined	(266489/266489/266489, 0/0/0)	[1.00002, 99.9998]	[-9.11001, 262.701]	[-9.95681, 160.428]
EGO	PCE PC p=4	Combined	(420/420/420, 0/0/0)	[1.00002, 99.9998]	[-3.35535, 1.66796]	[-2.65216, 1.09272]
EGO	PCE PC p=6	Combined	(1848/1848/1848, 0/0/0)	[1.00002, 99.9998]	[-7.85646, 3.94742]	[-5.22114, 9.56123]
EGO	PCE PC p=8	Combined	(6006/6006/6006, 0/0/0)	[1.00002, 99.9998]	[-6.82211, 2.37481]	[-4.98694, 5.05946]
EGO	SC SSG w=1	Aleatory	(108/171/378, 0/0/0)	[1.00002, 99.9998]	[-9.01837, 406.164]	[-9.68682, 1417.22]
EGO	SC SSG w=2	Aleatory	(588/931/1960, 0/0/0)	[1.00002, 99.9998]	[-8.99211, 404.962]	[-9.63453, 1409.56]
EGO	SC SSG w=3	Aleatory	(2412/3819/8040, 0/0/0)	[1.00002, 99.9998]	[-8.99211, 404.962]	[-9.63448, 1409.55]
EGO	SC SSG w=4	Aleatory	(8172/12939/27240, 0/0/0)	[1.00002, 99.9998]	[-8.99211, 404.962]	[-9.63448, 1409.56]
EGO	SC SSG w=4	Combined	(2381/2381/2381, 0)	[1.00002, 99.9998]	[-1.26801, ∞]	[-1.95236, ∞]
EGO	SC SSG w=6	Combined	(30869/30869/30869, 0)	[1.00002, 99.9998]	[-10.0003, ∞]	[-2.25563, ∞]
EGO	SC SSG w=8	Combined	(266489/266489/266489, 0)	[1.00002, 99.9998]	[-9.14279, 1479.76]	[-2.23834, ∞]
NPSOL	PCE SSG w=1	Aleatory	(27/45/27, 27/45/27)	[1.00000, 100.000]	[-9.03007, 406.393]	[-9.69101, 1417.85]
NPSOL	PCE SSG w=2	Aleatory	(147/245/147, 147/245/147)	[1.00000, 100.000]	[-8.99855, 404.970]	[-9.63476, 1409.62]
NPSOL	PCE SSG w=3	Aleatory	(603/1005/603, 603/1005/603)	[1.00000, 100.000]	[-8.99846, 404.966]	[-9.63449, 1409.58]
NPSOL	PCE SSG w=4	Aleatory	(2043/3405/2043, 2043/3405/2043)	[1.00000, 100.000]	[-8.99846, 404.966]	[-9.63449, 1409.58]
NPSOL	PCE SSG w=4	Combined	(2381/2381/2381, 0/0/0)	[1.00000, 100.000]	[11.1547, 28.4187]	[0.195964, 13.9033]
NPSOL	PCE SSG w=6	Combined	(30869/30869/30869, 0/0/0)	[1.00000, 100.000]	[-9.83785, 204.271]	[11.8015, 52.6142]
NPSOL	PCE SSG w=8	Combined	(266489/266489/266489, 0/0/0)	[1.00000, 100.000]	[-9.11003, 262.716]	[-9.95684, 151.372]
NPSOL	SC SSG w=1	Aleatory	(27/45/27, 27/45/27)	[1.00000, 100.000]	[-9.02482, 406.167]	[-9.68682, 1417.22]
NPSOL	SC SSG w=2	Aleatory	(147/245/147, 147/245/147)	[1.00000, 100.000]	[-8.99846, 404.966]	[-9.63453, 1409.57]
NPSOL	SC SSG w=3	Aleatory	(603/1005/603, 603/1005/603)	[1.00000, 100.000]	[-8.99846, 404.965]	[-9.63449, 1409.56]
NPSOL	SC SSG w=4	Aleatory	(2043/3405/2043, 2043/3405/2043)	[1.00000, 100.000]	[-8.99846, 404.965]	[-9.63449, 1409.56]
NPSOL	SC SSG w=4	Combined	(2381/2381/2381, 0/0/0)	[1.00000, 100.000]	[-13.7392, ∞]	[-16.0560, ∞]
NPSOL	SC SSG w=6	Combined	(30869/30869/30869, 0/0/0)	[1.00000, 100.000]	[-10.0004, ∞]	[-10.9630, ∞]
NPSOL	SC SSG w=8	Combined	(266489/266489/266489, 0/0/0)	[1.00000, 100.000]	[-9.14282, 1482.83]	[-9.88943, ∞]
LHS 100	LHS 100	N/A	(10^4/10^4/10^4, 0/0/0)	[1.69100, 88.0090]	[-8.31258, 324.114]	[-9.34799, 1119.22]
LHS 1000	LHS 1000	N/A	(10^6/10^6/10^6, 0/0/0)	[1.18837, 96.1182]	[-8.85165, 381.884]	[-9.55299, 1304.75]
LHS 10^4	LHS 10^4	N/A	(10^8/10^8/10^8, 0/0/0)	[1.11023, 98.8855]	[-8.96612, 398.167]	[-9.59256, 1376.45]

To again investigate the issue of degraded convergence rates for combined expansions, Figure 4.6 shows a comparison of convergence rates for L_2 versus L_∞ metrics for the cantilever beam problem, where all six variables are used in combined expansions. The L_∞ metrics are the β intervals shown previously in Table 4.2. For the L_2 case, all six variables are treated as aleatory and convergence in β value is shown. It is evident that L_2 convergence rates are again more rapid than L_∞ (approximately four orders of magnitude residual reduction compared to, at best, approximately two orders of reduction).

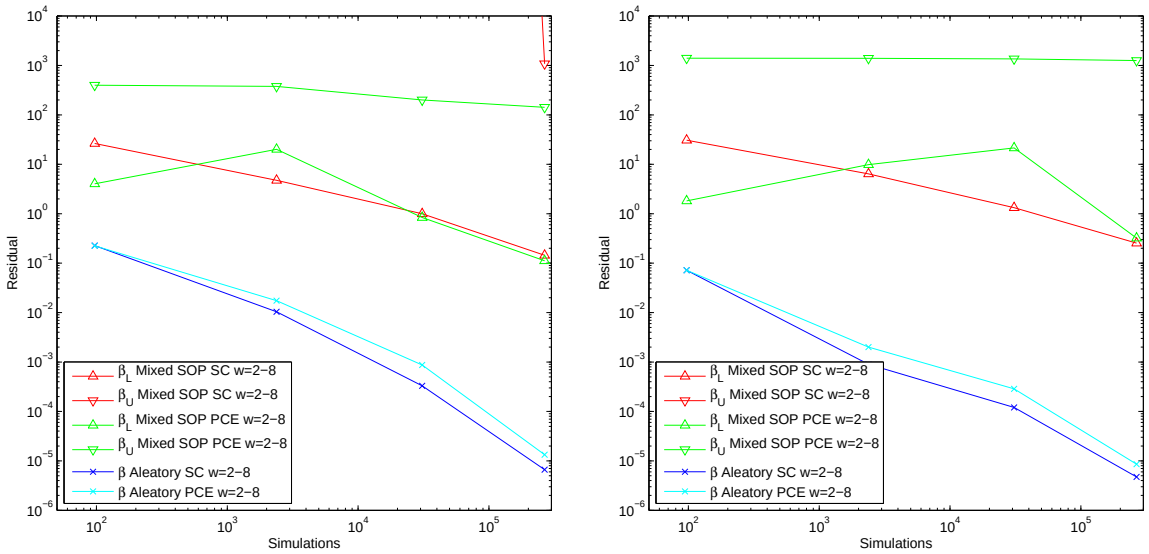

(a) Scaled stress.

(b) Scaled displacement.

Figure 4.6. Convergence rates for combined expansions in the cantilever beam test problem.

4.3 Ishigami

The previous two test functions are rational functions with limited regularity, which can degrade convergence rates in polynomial approximations. The Ishigami test problem [41] is a smooth C^∞ function:

$$f(\mathbf{x}) = \sin(2x_1 - \pi) + 7\sin^2(2\pi x_2 - \pi) + 0.1(2\pi x_3 - \pi)^4 \sin(2\pi x_1 - \pi) \qquad (4.4)$$

The distributions for x_1, x_2, and x_3 are *iid* uniform on [0,1]. A linear scaling transformation is applied and Legendre orthogonal polynomials are employed in the transformed space.

4.3.1 Epistemic interval estimation

In Figure 4.7, a comparison of convergence rates is shown for L_2 versus L_∞ metrics for the Ishigami problem, where all three variables are used in combined expansions. For the L_2 case, all three variables are treated as aleatory and convergence in β value is shown. For the L_∞ case, x_1 is treated as an epistemic interval while x_2 and x_3 remain aleatory, and convergence in the epistemic interval bounds for the aleatory β statistic is shown (in this case, all interval estimation is just post-processing of the combined expansion). It is evident that L_2 and L_∞ convergence rates are quite similar for this smooth C^∞ function: SC convergence plots are nearly on top of one another and the PCE convergence plots have a fairly consistent residual gap throughout. Thus, it appears that point-wise L_∞ accuracy can be achieved at similar cost to L_2 accuracy, provided that the function is sufficiently smooth.

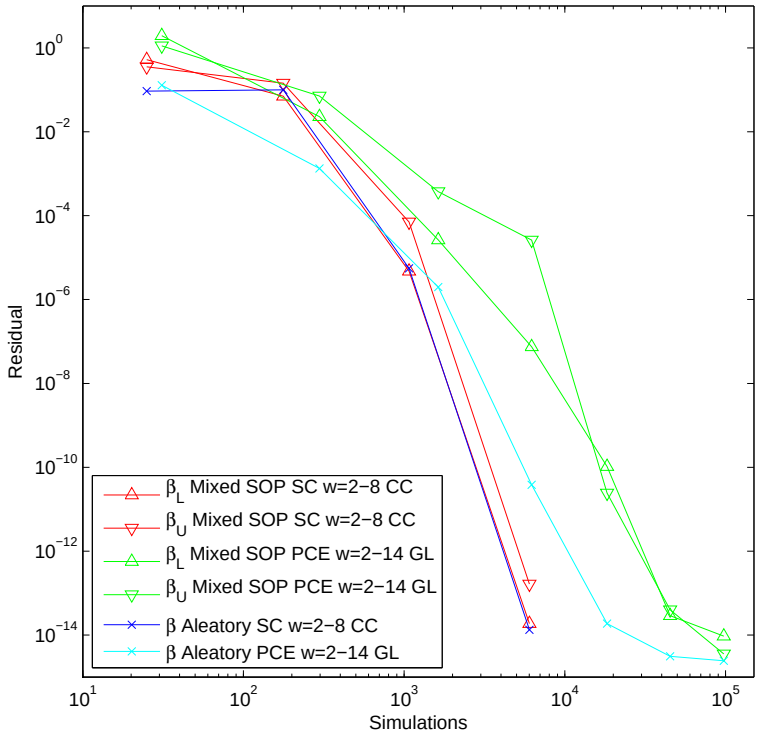

Figure 4.7. Convergence rates for combined expansions in the Ishigami test problem.

4.4 Sobol's g function

At the opposite end of the smoothness spectrum, Sobol's g-function [41] is C^0 with the absolute value contributing a slope discontinuity at the center of the domain:

$$f(\mathbf{x}) = 2\prod_{j=1}^{5} \frac{|4x_j - 2| + a_j}{1 + a_j}; \quad a = [0, 1, 2, 4, 8] \tag{4.5}$$

The distributions for x_j for $j = 1, 2, 3, 4, 5$ are *iid* uniform on [0,1]. A linear scaling transformation is applied and Legendre orthogonal polynomials are employed in the transformed space.

Without any mitigation measures (e.g., discretization of the random domain), we expect for smooth global polynomial approximations to exhibit Gibbs phenomena near the discontinuity, resulting in slow convergence in L_2 measures.

4.4.1 Epistemic interval estimation

In Figure 4.8, a comparison of convergence behavior is shown for L_2 versus L_∞ metrics for the Sobol g-function problem, where all five variables are used in combined expansions. Since convergence rates are relatively poor in this case, an overkill reference solution is not available and residuals cannot be reliably estimated. Rather, the values of the statistics are plotted directly and general convergence trends are inferred. For the L_2 case, all five variables are treated as aleatory and slow convergence in β value is apparent with agreement between the PCE and SC estimates. For the L_∞ case, x_1 and x_2 are treated as epistemic intervals while x_3 through x_5 remain aleatory and the resulting L_∞ intervals can be seen to be neither converging nor consistent between PCE and SC. Thus, one can infer that point-wise L_∞ accuracy may not be attainable for nonsmooth functions. In fact, one might anticipate divergence in some L_∞ metrics in the presence of Gibbs oscillations of increasing amplitude.

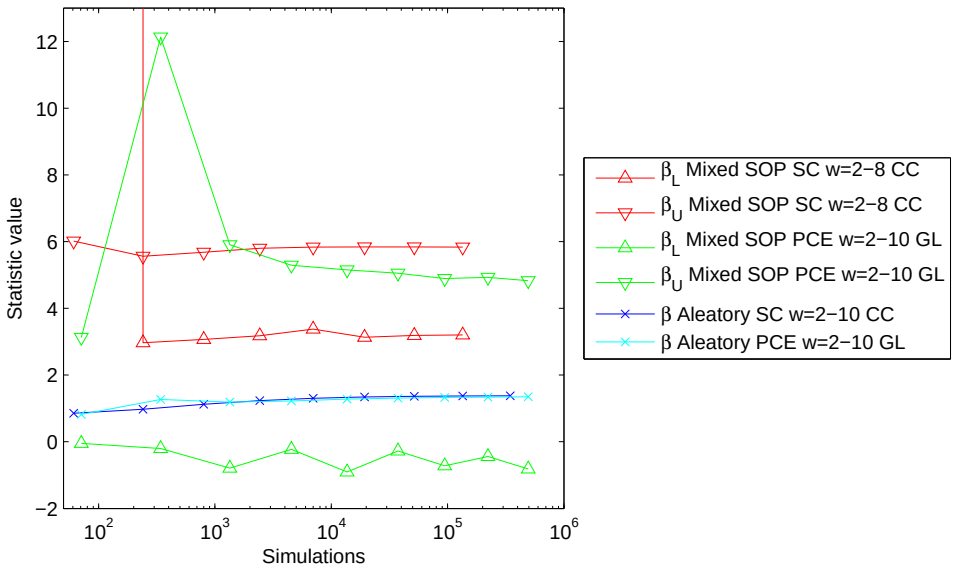

Figure 4.8. Convergence for combined expansions in the Sobol g-function test problem.

Chapter 5

Accomplishments and Conclusions

The goal of this milestone was to develop second-order probability approaches for mixed aleatory-epistemic uncertainty quantification that can be more accurate (via precise bounds from optimizers) and more efficient (via exponential convergence rates from stochastic expansion methods) than nested sampling. Computational experiments have demonstrated that the coupling of local gradient-based and global nongradient-based optimizers with nonintrusive polynomial chaos and stochastic collocation expansion methods is highly effective, and provides interval bounds on statistics for two model problems using $O(10^2) - O(10^3)$ simulations that are significantly more accurate than those obtainable from $O(10^8)$ simulations in the traditional nested sampling approach.

5.1 Observations on optimization-based interval estimation

While there are many different possible optimization algorithms that could be examined, we focused on two: the global nongradient-based EGO algorithm, based on successive refinement of Gaussian process surrogate models, and the local gradient-based NPSOL algorithm, employing stochastic sensitivities. Key considerations in these selections include data reuse between interval minimization and maximization steps, support for nonsmooth and/or multimodal response functions, and scalability to large numbers of epistemic parameters. For the first two considerations, global methods are more effective, and for the last consideration, local methods are more effective. Table 5.1 provides additional details.

Additional observations for optimization-based interval estimation include:

- In addition to EGO, global methods supporting data reuse include DIRECT (reuse of box partitioning data within minimization and maximization Pareto frontiers) and other global surrogate-based approaches. DIRECT will be of future interest since it avoids potential issues with Gaussian process ill-conditioning, scaling, etc.

Table 5.1. Comparison of local and global optimization-based interval estimation.

Algorithm Type	Pro	Con
Global	• Global data reuse • Responses may be multimodal and nonsmooth • Gradients not required	• Supports only up to $O(10^1)$ epistemic variables • "Soft" convergence is not as precise
Local	• Epistemic dimension may be large scale • "Hard" convergence at KKT points to tight precision	• Only initial point reuse • Response should be smooth and unimodal • Gradients should be accurate and reliable

- Another attractive future method would be EGO employing gradients (utilizing the concept of "gradient-based kriging"). This would retain the desirable global identification properties of EGO, but take advantage of the stochastic sensitivity capabilities to improve the accuracy of the Gaussian process models in order to accelerate the epistemic search. This would likely also mitigate epistemic dimensionality issues to some degree.

5.2 Observations on stochastic expansions

This report has included investigation of the relative performance of non-intrusive generalized polynomial chaos and Lagrange interpolation-based stochastic collocation methods applied to algebraic benchmark problems with known solutions. The primary distinction between these methods is that PCE must estimate coefficients for a known basis of orthogonal polynomials (using sampling, linear regression, tensor-product quadrature (TPQ), or Smolyak sparse grids (SSG)) whereas SC must form an interpolant for known coefficients (using TPQ or SSG).

Performance between these methods is shown to be very similar and both demonstrate impressive efficiency relative to Monte Carlo sampling methods and impressive accuracy relative to local reliability methods, thereby providing a more effective balance of accuracy and efficiency over current production UQ methods for aleatory uncertainty. When a difference is observed between traditional PCE and SC using the same collocation point sets, SC has been the consistent winner, typically manifesting in the reduction of the required integration by one order or level. This difference can be

attributed at least in part to expansion/integration synchronization issues with PCE, motivating approaches for tailoring of chaos expansions that closely synchronize with numerical integration schemes:

- For the case of TPQ, tailored tensor-product PCE is shown to perform identically to SC such that the performance gap is completely eliminated. Both methods consistently outperform traditional total-order PCE. However, TPQ approaches only outperform SSG approaches for the lowest dimensional problems.
- For problems with greater than two dimensions, SSG approaches are shown to outperform TPQ approaches.
  - For SSG, selection of a synchronized PCE formulation is nontrivial and the tailored total-order PCE approach, which computes the maximal total-order expansion that can be resolved by a particular SSG, is shown to be more rigorous and reliable than heuristics and eliminates inefficiency due to trial and error.
  - A significant performance gap relative to SC with SSG still remains for the case of nonlinear growth rules, but replacement of these rules with linear ones (for Gaussian quadratures that are at most weakly nested) reduces the set of resolvable monomials that do not appear in the total-order expansion, resulting in a further reduction of the performance gap.

While efforts in tailoring the form of the PCE can reduce and in some cases eliminate the performance gap with SC, no nonintrusive PCE approach has been shown to outperform SC when using the same set of collocation points. Rather, usage of PCE remains motivated by other considerations, in particular its greater flexibility in collocation point selection and coefficient estimation approaches. In particular, PCE allows for:

- usage of unstructured/random collocation point sets (with random sampling and linear regression approaches) that can support greater simulation fault tolerance
- Genz cubature grids that support more optimal numerical integration than SSG, at least for low order rules
- linear regression approaches that may enable approximate resolution of higher random dimensions and higher expansion orders than SSG approaches

In addition, a guarantee of positive expansion variance is a feature of PCE not provided by SC, and this can be particularly important when computing intervals on variance-related metrics. Thus, PCE and SC provide their own sets of strengths

and weaknesses and selection between the two approaches remains dependent on the efficiency and flexibility requirements of specific applications.

Another type of stochastic expansion tailoring that was explored is the selection of basis polynomials along with their associated Gauss points and weights. For independent random variables with density functions outside of the Askey family, two approaches are supported: (1) nonlinear variable transformation of the non-Askey density function to the most similar Askey density, or (2) numerical generation of polynomials that are orthogonal with respect to an arbitrary density. Mixed results were shown in which simple polynomial response functions showed clear benefit from the numerically-generated basis, but rational response functions with non-Askey variables in the denominator required lower order response expansions using the variable transformation approach. It is expected that the special conditions met in the rational function examples will be the exception rather than the rule, and that numerically generated polynomials will generally be preferred; however, additional computational experience is needed.

5.3 Observations on second-order probability

The preferred UQ approaches identified in stochastic expansion computational experiments are (1) SC with TPQ for low dimensions and linear growth SSG for high dimensions, and (2) tailored PCE with TPQ for low dimensions and either linear growth SSG or linear regression for high dimensions. These approaches are carried forward in epistemic interval estimation studies employing two stochastic expansion/sensitivity approaches (aleatory and combined expansions) and two optimization approaches (local gradient-based and global nongradient-based).

For the expansion/sensitivity approaches, the first approach forms expansions only over the aleatory uncertain variables for both the response values and the response sensitivities. It is a first-order technique requiring accurate derivatives of the response function with respect to the epistemic variables; derivatives of aleatory statistics with respect to epistemic variables are formed based on aleatory expectations of epistemic response derivatives. The second approach forms combined expansions of response values over both the aleatory and epistemic variables. It is a zeroth-order technique; derivatives of statistics are formed by differentiating the polynomial relationship between the aleatory statistics (formed from integrating out the aleatory expansion terms) and the remaining epistemic expansion terms. While it is shown that both approaches are capable of exact results, computational experiments indicate that the former aleatory expansion approach is generally more efficient and reliable (so long as the underlying epistemic response derivatives are reliable) for use within optimization-based interval estimation. This appears to be due to two factors:

1. Convergence rates can be degraded when computing point-wise L_∞ metrics

(minima and maxima) from stochastic expansions. Rational, infinitely differentiable, and discontinuous response functions were investigated, and only for the smooth C^∞ case were the L_2 and L_∞ convergence rates comparable. Thus, for general functions that may not be infinitely differentiable, it appears preferable to restrict stochastic expansion approximation to dimensions requiring aleatory L_2 metrics (mean, variance, probability) and to handle dimensions requiring epistemic L_∞ metrics (interval bounds) through other means (i.e., direct optimization without stochastic expansion approximation).

2. The previous statement assumes sparse interrogation of the epistemic space by efficient local and global optimizers. For second-order probability in which a single interval is computed for each response function, the number of epistemic point evaluations is relatively small, such that the cost of resolving the aleatory statistics for only selected instances of the nonprobabilistic parameters (aleatory expansions) one at a time may tend to be more efficient than attempting to globally resolve these statistics for all values of the nonprobabilistic parameters (combined expansions) all at once. For more finely-discretized epistemic analyses such as Dempster-Shafer theory of evidence, the interrogation requirements for the epistemic space may grow substantially, such that combined expansions may prove useful in this case. Moreover, development of more rapidly converging approaches in L_∞ for combined expansions may be possible and may become motivated by the Dempster-Shafer use case.

For the optimization approaches, the first approach employs the stochastic sensitivities from the aleatory or combined expansions to perform a local gradient-based search for minima and maxima of the response metrics over the epistemic parameter ranges. As for all local gradient-based methods (and as discussed previously in Section 5.1), it requires response metrics that are smooth and unimodal over the epistemic space to be effective. The second approach employs a nongradient-based global search for minima and maxima. It is a zeroth-order technique that only requires accurate predictions of the aleatory statistic values over the epistemic space. In both the short column and cantilever beam test problems, the aleatory statistics behaved monotonically over the epistemic parameter ranges, such that both local and global searches located the same solutions. For the short column problem, the expense of the best local and global approaches was comparable (341 limit state function and gradient evaluations for NPSOL versus 403 limit state function evaluations for EGO); whereas in the cantilever beam problem, the local search displayed greater efficiency (245 stress and 147 displacement function/gradient evaluations for NPSOL versus 931 stress and 1960 displacement function evaluations for EGO). Overall, these experiments are consistent with the anticipated trade-off between the scalability and efficiency of local approaches and the robustness of global approaches for nonsmooth, multimodal problems; although additional experimentation will help quantify these effects more precisely. Relative to nested sampling in the short column problem, our new approaches reduce expense by greater than five orders of magnitude while achieving more precise results (five to six digits of accuracy in the output intervals

instead of only one to three digits). And in the cantilever beam problem, our new approaches are again much more efficient, reducing expense by five to six orders of magnitude, while again achieving more precise results, four to six digits of accuracy instead of only zero to two.

Additional observations include:

- Since the relative computational expense of the local and global optimization approaches is only relevant for point-wise aleatory expansions, the greater algorithmic robustness of the global EGO approach is recommended for interval estimation on combined expansions, since these expansions only involve inexpensive post-processing in either optimization case.

- Overall, the most effective SOP approach was SC using linear SSG with expansions formed only over the aleatory variables for each instance of the epistemic variables. In this case, the selection between local and global optimization is relevant and should be based on the efficiency, scalability, and algorithmic robustness concerns previously identified.

- This report explored global-global and local-global combinations for outer-inner nested loops to support either algorithmic robustness or scalability with respect to epistemic dimension. To sacrifice algorithmic robustness in exchange for scalability with respect to aleatory dimension, global stochastic expansions could be replaced with local gradient-based reliability methods for aleatory UQ. Overall, global-global, local-global, global-local, and local-local combinations are all easily configured in DAKOTA, allowing one to tailor the approach for robustness or scalability separately within epistemic and aleatory domains.

- In future research, dimension-adaptive stochastic expansion methods will better address the curse of dimensionality, allowing usage of global machinery at reduced cost for larger problems.

5.4 Accomplishments, Capability Development, and Deployment

This milestone crosscuts multiple centers, drawing on capabilities for uncertainty analysis from DAKOTA (1410), device and circuit simulation from Charon and Xyce (1430), and QASPR data analysis, model development, and program relevance (0410, 1340, 1430, 1540). Many new capabilities have been developed and tested within the DAKOTA code for use in this milestone, including:

- stochastic expansions over nonprobabilistic dimensions

- stochastic sensitivity analysis capabilities for aleatory and combined expansions
- local gradient-based and global nongradient-based optimization approaches to epistemic interval estimation with data reuse among minimization and maximization solves
- nested analyses within second-order probability and Dempster-Shafer methods for mixed aleatory-epistemic UQ

New capabilities developed for this milestone are being inserted into production UQ analysis procedures for current and future radiation effects studies, and this trend is expected to continue with V&V efforts in other program areas.

References

[1] M. Abramowitz and I. A. Stegun. *Handbook of Mathematical Functions with Formulas, Graphs, and Mathematical Tables*. Dover, New York, 1965.

[2] R. Askey and J. Wilson. Some basic hypergeometric polynomials that generalize jacobi polynomials. In *Mem. Amer. Math. Soc. 319*, Providence, RI, 1985. AMS.

[3] V. Barthelmann, E. Novak, and K. Ritter. High dimensional polynomial interpolation on sparse grids. *Adv. Comput. Math.*, 12(4):273–288, 2000. Multivariate polynomial interpolation.

[4] B. J. Bichon, M. S. Eldred, L. P. Swiler, S. Mahadevan, and J. M. McFarland. Efficient global reliability analysis for nonlinear implicit performance functions. *AIAA Journal*, 46(10):2459–2468, 2008.

[5] G. E. P. Box and D. R Cox. An analysis of transformations. *J. Royal Stat. Soc.*, 26:211–252, 1964.

[6] X. Chen and N .C. Lind. Fast probability integration by three-parameter normal tail approximation. *Struct. Saf.*, 1:269–276, 1983.

[7] A. Der Kiureghian and P. L. Liu. Structural reliability under incomplete probability information. *J. Eng. Mech., ASCE*, 112(1):85–104, 1986.

[8] M. S. Eldred. Recent advances in non-intrusive polynomial chaos and stochastic collocation methods for uncertainty analysis and design. In *Proceedings of the 11th AIAA Nondeterministic Approaches Conference*, number AIAA-2009-2274, Palm Springs, CA, May 4–7 2009.

[9] M. S. Eldred, B. M. Adams, K. Haskell, W. J. Bohnhoff, J. P. Eddy, D. M. Gay, W. E. Hart, P. D. Hough, T. G. Kolda, L. P. Swiler, and J.-P. Watson. DAKOTA, a multilevel parallel object-oriented framework for design optimization, parameter estimation, uncertainty quantification, and sensitivity analysis: Version 4.2 users manual. Technical Report SAND2006-6337, Sandia National Laboratories, Albuquerque, NM, 2008.

[10] M. S. Eldred, H. Agarwal, V. M. Perez, S. F. Wojtkiewicz, Jr., and J. E. Renaud. Investigation of reliability method formulations in DAKOTA/UQ. *Structure & Infrastructure Engineering: Maintenance, Management, Life-Cycle Design & Performance*, 3(3):199–213, 2007.

[11] M. S. Eldred and B. J. Bichon. Second-order reliability formulations in DAKOTA/UQ. In *Proceedings of the 47th AIAA/ASME/ASCE/AHS/ASC Structures, Structural Dynamics and Materials Conference*, number AIAA-2006-1828, Newport, RI, May 1–4 2006.

[12] M. S. Eldred and J. Burkardt. Comparison of non-intrusive polynomial chaos and stochastic collocation methods for uncertainty quantification. In *Proceedings of the 47th AIAA Aerospace Sciences Meeting and Exhibit*, number AIAA-2009-0976, Orlando, FL, January 5–8, 2009.

[13] M. S. Eldred and D. M. Dunlavy. Formulations for surrogate-based optimization with data fit, multifidelity, and reduced-order models. In *Proceedings of the 11th AIAA/ISSMO Multidisciplinary Analysis and Optimization Conference*, number AIAA-2006-7117, Portsmouth, VA, September 6–8 2006.

[14] M. S. Eldred, C. G. Webster, and P. Constantine. Design under uncertainty employing stochastic expansion methods. In *Proceedings of the 12th AIAA/ISSMO Multidisciplinary Analysis and Optimization Conference*, number AIAA-2008-6001, Victoria, British Columbia, September 10–12, 2008.

[15] M. S. Eldred, C. G. Webster, and P. Constantine. Evaluation of non-intrusive approaches for wiener-askey generalized polynomial chaos. In *Proceedings of the 10th AIAA Nondeterministic Approaches Conference*, number AIAA-2008-1892, Schaumburg, IL, April 7–10 2008.

[16] P. Frauenfelder, C. Schwab, and R. A. Todor. Finite elements for elliptic problems with stochastic coefficients. *Comput. Methods Appl. Mech. Engrg.*, 194(2-5):205–228, 2005.

[17] J. M Gablonsky. An implementation of the direct algorithm. Technical Report Technical Report CRSC-TR98-29, Center for Research in Scientific Computation, North Carolina State University, Chapel Hill, NC, August 1998.

[18] W. Gautschi. *Orthogonal Polynomials: Computation and Approximation*. Oxford University Press, New York, 2004.

[19] T. Gerstner and M. Griebel. Numerical integration using sparse grids. *Numer. Algorithms*, 18(3-4):209–232, 1998.

[20] R. G. Ghanem. private communication.

[21] P. E. Gill, W. Murray, M. A. Saunders, and M. H. Wright. User's guide for npsol 5.0: A fortran package for nonlinear programming. Technical Report SOL 86-1, System Optimization Laboratory, Stanford University, Stanford, CA, Revised July 1998.

[22] G. H.. Golub and J. H. Welsch. Caclulation of gauss quadrature rules. *Mathematics of Computation*, 23(106):221–230, 1969.

[23] J. C. Helton. Conceptual and computational basis for the quantification of margins and uncertainty. Technical Report SAND2009-3055, Sandia National Laboratories, Albuquerque, NM, July 2009.

[24] J. C. Helton, J. D. Johnson, and W. L. Oberkampf. An exploration of alternative approaches to the representation of uncertainty in model predictions. *Reliability Engineering and System Safety*, 85:39–71, 2004.

[25] J. C. Helton, J. D. Johnson, W. L. Oberkampf, and C. B. Storlie. A sampling-based computational strategy for the representation of epistemic uncertainty in model predictions with evidence theory. *Computer Methods in Applied Mechanics and Engineering*, 196:3980–3998, 2007.

[26] S. Hosder, R. W. Walters, and M. Balch. Efficient sampling for non-intrusive polynomial chaos applications with multiple uncertain input variables. In *Proceedings of the 48th AIAA/ASME/ASCE/AHS/ASC Structures, Structural Dynamics, and Materials Conference*, number AIAA-2007-1939, Honolulu, HI, April 23–26, 2007.

[27] D. Huang, T. T. Allen, W. I. Notz, and N. Zang. Global optimization of stochastic black-box systems via sequential kriging meta-models. *J. Global Optimization*, 34:441–466, 2006.

[28] D. Jones, M. Schonlau, and W. Welch. Efficient global optimization of expensive black-box functions. *J. Global Optimization*, 13:455–492, 1998.

[29] N. Kuschel and R. Rackwitz. Two basic problems in reliability-based structural optimization. *Math. Method Oper. Res.*, 46:309–333, 1997.

[30] J. D. Martin and T. W. Simpson. Use of kriging models to approximate deterministic computer models. *AIAA Journal*, 43(4):853–863, 2005.

[31] J. M. McFarland. *Uncertainty Analysis for Computer Simulations through Validation and Calibration*. PhD thesis, Vanderbilt University, Nashville, TN, May 2008.

[32] J. C. Meza. OPT++: An object-oriented class library for nonlinear optimization. Technical Report SAND94-8225, Sandia National Laboratories, Albuquerque, NM, March 1994.

[33] F. Nobile, R. Tempone, and C. G. Webster. An anisotropic sparse grid stochastic collocation method for partial differential equations with random input data. *SIAM J. on Num. Anal.*, 2008. To appear.

[34] F. Nobile, R. Tempone, and C. G. Webster. A sparse grid stochastic collocation method for partial differential equations with random input data. *SIAM J. on Num. Anal.*, 2008. To appear.

[35] R. Rackwitz and B. Fiessler. Structural reliability under combined random load sequences. *Comput. Struct.*, 9:489–494, 1978.

[36] M. T. Reagan, H. N. Najm, P. P. Pebay, O. M. Knio, and R. G. Ghanem. Quantifying uncertainty in chemical systems modeling. *Int. J. Chem. Kinet.*, 37:368–382, 2005.

[37] M. Rosenblatt. Remarks on a multivariate transformation. *Ann. Math. Stat.*, 23(3):470–472, 1952.

[38] J. Sacks, S. B. Schiller, and W. Welch. Design for computer experiments. *Technometrics*, 31:41–47, 1989.

[39] I.C. Simpson. Numerical integration over a semi-infinite interval, using the log-normal distibution. *Numerische Mathematik*, 31, 1978.

[40] S.A. Smolyak. Quadrature and interpolation formulas for tensor products of certain classes of functions. *Dokl. Akad. Nauk SSSR*, 4:240–243, 1963.

[41] C. B. Storlie, L. P. Swiler, J. C. Helton, and C. J. Sallaberry. Implementation and evaluation of nonparametric regression procedures for sensitivity analysis of computationally demanding models. *Reliability Engineering and System Safety*, 94:1735–1763, 2009.

[42] B. Sudret. Global sensitivity analysis using polynomial chaos expansions. *Reliability Engineering and System Safety*, 93, 2008.

[43] R. Sues, M. Aminpour, and Y. Shin. Reliability-based multidisciplinary optimization for aerospace systems. In *Proceedings of the 42rd AIAA/ASME/ASCE/AHS/ASC Structures, Structural Dynamics, and Materials Conference*, number AIAA-2001-1521, Seattle, WA, April 16–19, 2001.

[44] L. P. Swiler, T. L. Paez, and R. L. Mayes. Epistemic uncertainty quantification tutorial. In *Proceedings of the IMAC XXVII Conference and Exposition on Structural Dynamics*, number paper 294, Orlando, FL, February 2009.

[45] L. P. Swiler, T. L. Paez, R. L. Mayes, and M. S. Eldred. Epistemic uncertainty in the calculation of margins. *Proceedings of the 50th AIAA/ASME/ASCE/AHS/ASC Structures, Structural Dynamics, and Materials Conference*, (AIAA-2009-2249), May 4-7, 2009.

[46] G. Tang, G. Iaccarino, and M. S. Eldred. Global sensitivity analysis for stochastic collocation expansion. In *abstract submitted for 12th AIAA Non-Deterministic Approaches Conference*, Orlando, FL, April 12–15, 2010.

[47] G. Tang, L. P. Swiler, and M. S. Eldred. Using stochastic expansion methods in evidence theory for mixed aleatory-epistemic uncertainty quantification. In *abstract submitted for 12th AIAA Non-Deterministic Approaches Conference*, Orlando, FL, April 12–15, 2010.

[48] R. W. Walters. Towards stochastic fluid mechanics via polynomial chaos. In *Proceedings of the 41st AIAA Aerospace Sciences Meeting and Exhibit*, number AIAA-2003-0413, Reno, NV, January 6–9, 2003.

[49] G. W. Wasilkowski and H. Woźniakowski. Explicit cost bounds of algorithms for multivariate tensor product problems. *Journal of Complexity*, 11:1–56, 1995.

[50] N. Wiener. The homogoeneous chaos. *Amer. J. Math.*, 60:897–936, 1938.

[51] J. A. S. Witteveen and H. Bijl. Modeling arbitrary uncertainties using gram-schmidt polynomial chaos. In *Proceedings of the 44th AIAA Aerospace Sciences Meeting and Exhibit*, number AIAA-2006-0896, Reno, NV, January 9–12 2006.

[52] Y.-T. Wu, Y. Shin, R. Sues, and M. Cesare. Safety-factor based approach for probability-based design optimization. In *Proceedings of the 42rd AIAA/ASME/ASCE/AHS/ASC Structures, Structural Dynamics, and Materials Conference*, number AIAA-2001-1522, Seattle, WA, April 16–19, 2001.

[53] Y.-T. Wu and P. H. Wirsching. A new algorithm for structural reliability estimation. *J. Eng. Mech., ASCE*, 113:1319–1336, 1987.

[54] D. Xiu and J.S. Hesthaven. High-order collocation methods for differential equations with random inputs. *SIAM J. Sci. Comput.*, 27(3):1118–1139 (electronic), 2005.

[55] D. Xiu and G. M. Karniadakis. The wiener-askey polynomial chaos for stochastic differential equations. *SIAM J. Sci. Comput.*, 24(2):619–644, 2002.

DISTRIBUTION:

1 Juan J. Alonso
Durand Building, Room 365
Department of Aeronautics & Astronautics
Stanford University
Stanford, CA 94305

1 Barron J. Bichon
Research Engineer
Southwest Research Institute
6220 Culebra Road
P.O. Drawer 28510
San Antonio, Texas 78228-0510

1 Krzysztof J. Fidkowski
Department of Aerospace Engineering
The University of Michigan
3029 FXB Building
Ann Arbor, MI 48109

1 Roger Ghanem
254C Kaprielian Hall
Dept. of Civil Engineering
3620 S. Vermont Ave.
University of Southern California
Los Angeles, CA 90089-2531

1 Raphael Haftka
Dept. of Aerospace and Mechanical Engineering and Engineering Science
P.O. Box 116250
University of Florida
Gainesville, FL 32611-6250

1 Gianluca Iaccarino
Bldg 500, 500-I, Mechanical Engineering Department
Institute for Computational Mathematical Engineering
Stanford University
Stanford, CA 94305-3030

1 Sankaran Mahadevan
Department of Civil and Environmental Engineering
Box 1831, Station B
Vanderbilt University
Nashville, TN 37235

1 Kurt Maute
Department of Aerospace Engineering Sciences
University of Colorado at Boulder
Room ECAE 183, Campus Box 429
Boulder, Colorado 80309-0429

1 John E. Renaud
University of Notre Dame
Aerospace and Mechanical Engineering
365 Fitzpatrick Hall
Notre Dame, IN 46556-5637

1 Christopher J. Roy
215 Randolph Hall
Virginia Polytechnic Institute and State University
Blacksburg, Virginia 24061-0203

1 Karen E. Willcox
Department of Aeronautics & Astronautics
Massachusetts Institute of Technology
77 Massachusetts Ave
Room 37-447
Cambridge, MA 02139

1 Steven F. Wojtkiewicz, Jr.
Department of Civil Engineering
University of Minnesota
500 Pillsbury Drive S.E.
Minneapolis, MN 55455-0116

1 Dongbin Xiu
Math Department
Math 434
Purdue University
West Lafayette, IN 47907

5 Lawrence Livermore National Laboratory
7000 East Ave.
P.O. Box 808
Livermore, CA 94550
Attn: Scott Brandon, MS L-023
Frank Graziani, MS L-095
Richard Klein, MS L-023
Jim McEnerney, MS L-023
Charles Tong, MS L-560

3 Los Alamos National Laboratory
Mail Station 5000
P.O. Box 1663
Los Alamos, NM 87545
Attn: Marc Anderson, MS T080
Scott Doebling, MS T080
Francois Hemez, MS T006

1 MS 0316
J. P. Castro, 1437

1 MS 0316
R. J. Hoekstra, 1437

1 MS 0316
E. R. Keiter, 1437

1 MS 0316
B. S. Paskaleva, 1437

1 MS 0321
J. S. Peery, 1400

1 MS 0352
C. E. Hembree, 1344

1 MS 0370
T. G. Trucano, 1411

1 MS 0378
A. M. Robinson, 1431

1 MS 0380
G. M. Reese, 1542

1 MS 0380
D. E. Womble, 1540

1 MS 0382
B. Carnes, 1543

1 MS 0492
T. D. Brown, 0411

2 MS 0776
J. C. Helton, 1544

1 MS 0828
A. R. Black, 1544

1 MS 0828
K. J. Dowding, 1544

1 MS 0828
A. A. Giunta, 1544

1 MS 0828
R. G. Hills, 1544

1 MS 0828
M. Pilch, 1551

1 MS 0828
J. R. Red-Horse, 1544

1 MS 0828
V. J. Romero, 1544

1 MS 0829
B. M. Rutherford, 0415

1 MS 0836
M. M. Hopkins, 1514

1 MS 0836
P. K. Notz, 1514

1 MS 0847
R. V. Field, 1526

1 MS 1318
B. M. Adams, 1411

1 MS 1318
K. F. Alvin, 1414

3 MS 1318
M. S. Eldred, 1411

1 MS 1318
B. A. Hendrickson, 1410

1 MS 1318
R. P. Pawlowski, 1414

1 MS 1318
E. T. Phipps, 1411

1 MS 1318
J. R. Stewart, 1411

3 MS 1318
L. P. Swiler, 1411

1 MS 1320
S. S. Collis, 1416

1 MS 1322
J. B. Aidun, 1435

1 MS 1415
S. M. Meyers, 1110

1 MS 9051
B. J. Debusschere, 8351

1 MS 9051
H. N. Najm, 8351

1 MS 9159
H. R. Ammerlahn, 8962

1 MS 9159
G. A. Gray, 8964

1 MS 9159
P. D. Hough, 8964

1 MS 0899
Technical Library, 9536
(electronic copy)

Sandia National Laboratories